Source identification and temporal evolution of trace elements in PM 10 collected near to Ny-Ålesund (Norwegian Arctic)

Source identification and temporal evolution of trace elements in PM_{10} collected near to Ny-Ålesund (Norwegian Arctic)

E. Conca[a*], O. Abollino[a], A. Giacomino[b], S. Buoso[a], R. Traversi[c], S. Becagli[c], M. Grotti[d], M. Malandrino[a]

[a] *Department of Chemistry, University of Turin, Italy*
[b] *Department of Drug Science and Technology, University of Turin, Italy*
[c] *Department of Chemistry "Ugo Schiff", University of Florence, Italy*
[d] *Department of Chemistry and Industrial Chemistry, University of Genoa, Italy*
[*] *Corresponding author (eleonora.conca@unito.it; Via P. Giuria 5, 10125 Turin, Italy)*

Abstract: This study investigated the elemental composition of PM_{10} collected in a polar environment (Ny-Ålesund, Norwegian Arctic), to identify its sources and to understand the effects of short- and long-range transport processes. Natural (crustal and marine) and anthropogenic Arctic PM sources were identified, and specific emission sources were recognised by means of Principal Component Analysis and Hierarchical Cluster Analysis: airborne pollution deriving from ship fuels, local vehicle (non-exhaust) and continental emissions (e.g. incinerators or industries) were the main sources of anthropogenic elements. The results obtained so far from samples collected during four successive spring-summer sampling campaigns (2010-2013) show a remarkable seasonal trend for most of the investigated elements. For both geogenic and anthropogenic elements, concentrations are generally higher in March and April, when the ground is almost entirely covered by snow and ice, suggesting that long-range transport processes might be taking place. On the other hand, the concentrations of anthropogenic metals related to ship emissions (i.e. Co, Ni and V) peak in late spring and summer, when the marine traffic in the fjord is generally higher. For most of the analytes, the four campaigns were not significantly different; therefore, in the studied period, the composition of PM_{10} in Ny-Ålesund did not vary remarkably. Finally, the behaviour of Rare Earth Elements was discussed in terms of parent material mineralogy.

Keywords: Ny-Ålesund (Norwegian Arctic), PM_{10}, elemental composition, seasonal trends, enrichment factors, Principal Component Analysis

Declarations of interest: none.

1. Introduction

The ambient concentration and the chemical composition of atmospheric particulate matter (PM) depend on a large number of factors, such as the existence of specific sources (natural or anthropogenic) and the environmental conditions (season, weather and geographical area) (Minguillón et al., 2012). Conversely, PM is able to strongly influence the ongoing climate changes, by taking part in many atmospheric physical and chemical processes. Suspended particles can perturb the radiative balance of the atmosphere by means of both direct and indirect effects, e.g. the scattering and the absorption of the solar radiation and the tendency of particles to act as cloud condensation nuclei and to participate in cloud formation (Giardi et al., 2016; Moroni et al., 2016; Talbi et al., 2018). The link between PM and climate change is particularly important for polar regions since, in these areas, even small changes of PM concentration or composition can have significant effects on climate. In fact, polar regions play a key role in regulating the global biogeochemical cycles and hence the Earth's climate system. In the last few decades, global warming has caused a reduction of the polar sea-ice and snow cover. As a consequence, the capacity of the Earth's surface to reflect the solar radiation (albedo) has decreased, causing a further increase in temperatures. These complex feedback mechanisms cause fast climate changes, which result in poor process understanding and low-accuracy model predictions (Cappelletti et al., 2016).

The study of the chemical composition of polar PM is of great importance in aiding identification of local and global sources and transport mechanisms and potential for deposition in the Arctic. In winter and spring, when polluted air masses are more efficiently transported from mid-latitudes, various pollutants introduced in temperate zones reach the Arctic, giving rise to the so-called "Arctic haze" (Quinn et al., 2007). The composition of this haze includes sulphates, nitrates, ammonium, organic matter, black carbon and heavy metals (Barrie et al., 1992; Barrie and Hoff, 1985; Bodhaine et al., 1989; Clarke, 1989; Gong and Barrie, 2005; Udisti et al., 2016). The latter are among the chemical markers commonly used in source apportionment studies to identify the origin of PM (Bazzano et al., 2015; Bazzano et al., 2016a; Polissar and Hopke, 1998; Shaw, 1982; Talbi et al., 2018).

In order to gain a better understanding of the effects of short- and long-range transport processes taking place in this remote area, this study investigated the elemental composition of PM_{10} samples (aerodynamic diameter < 10 μm). The samples were collected at Gruvebadet Station, near to Ny-Ålesund (Svalbard Islands), during four subsequent spring-summer sampling campaigns (2010-2013). The choice of focussing on PM_{10} fraction was driven by the desire of evaluating the totality of the sources of Arctic PM and by the awareness that soil dust and particles deriving from non-exhaust vehicle emissions usually have a relatively high aerodynamic diameter. In addition, a reduction of the collected particles would probably have resulted in a higher proportion of results below the LOD, only allowing the determination of major elements. In fact, the total mass concentration of the suspended particles (TSP) previously found over the Arctic Ocean ranged from 0.10 to 3.8 $\mu g/m^3$ (Leck and Persson, 1996) and, in particular, an average of 0.61 $\mu g/m^3$ was registered in summer 2012 in Ny-Ålesund (Zhan et al., 2014). The concentrations of Al, As, Ba, Ca, Cd, Co, Cu, Fe, In, K, Mg, Mn, Mo, Na, Ni, Pb, Ti, V, Zn and most of lanthanides (also indicated as Rare Earth Elements or REEs), namely La, Ce, Pr, Nd, Sm, Eu, Gd, Tb, Dy, Ho, Er, Tm, Yb and Lu, was determined; all these elements are commonly used, with the aid of chemometric treatments and other graphical and statistical tools, as specific chemical markers for identifying the anthropogenic and natural (crustal and marine) sources of atmospheric PM. An adequate analytical procedure to determine the trace element content in PM collected in a virtually pristine area was developed and optimized; an Inductively Coupled Plasma - Optical Emission Spectrometer (ICP-OES) and a High-Resolution Inductively Coupled Plasma – Mass Spectrometer (HR-ICP-MS) were used for the analysis. The results obtained from samples collected in 2010 campaign have already been published (Bazzano et al., 2016a); in this work, results obtained from samples collected during 2011, 2012 and 2013 campaigns are presented, and comprehensive graphic and statistical treatments are shown.

2. Experimental

2.1 Study area and sampling

Ny-Ålesund (78°55'30"N, 11°55'40" E) is a small settlement acting as a centre for international Arctic scientific research and environmental monitoring. It is located on the shore of the bay of Kongsfjorden, on the western coast of Spitsbergen Island, in the Svalbard archipelago (Figure 1). The aerosol sampling was performed at Gruvebadet research station (40 m a.s.l.), situated at the base of Zeppelin Mountain (474 m a.s.l.), 800 m far from Ny-Ålesund. The location was established considering the prevailing wind direction (115° N) (Mazzola et al., 2016), in order to minimize the influence of local pollution during measurements. Moreover, a meteo-trigger system was used for switching off the sampling devices when the wind was absent (< 0.5 m/s) or came from Ny-Ålesund.

PM_{10} samples were collected with a 4-days resolution during four subsequent spring-summer sampling campaigns (2010-13), as indicated in Table 1. PTFE hydrophilic filters (Advantec, product code: H100A090C, 90 mm diameter, efficiency > 99% for 0.3 μm particles) and an Echo HiVol sampler (TCR Tecora, 200 L/min) were used. After each sampling, filters were placed in polycarbonate Petri dishes, sealed and immediately frozen; samples were maintained at -20°C during all stages of transportation to Italy and storage.

2.2 Apparatus and reagents

The dissolution of samples was carried out using a Milestone Ethos One microwave laboratory unit. Analyses were carried out using ICP-OES or HR-ICP-MS, according to the analyte concentration ranges; wavelength, mass resolution and isotope selection were optimized for each element to ensure resolution of spectral interferences and maximization of sensitivity. Table 2 reports model and feature of each instrumental technique used. Operating conditions and experimentally determined limits of detection (LOD) for all the elements determined in PM_{10} samples, are reported in Table 3; LOD values represent the analyte concentration (ppt or ppb) corresponding to three times the standard deviation of the reagent blank. LOD values reported in Table 3 in fg/m^3 and pg/m^3 were obtained by conversion, using the nominal air volume of 1152 m^3 and 15 mL as solution volume.

For the digestion of samples, ultrapure hydrogen peroxide (Sigma-Aldrich) and nitric acid (Fluka), further purified by sub-boiling distillation in a quartz apparatus, were used. Water was purified in a Milli-Q system, resulting in high purity water (HPW) with a resistivity of 18.2 MΩ·cm. Intermediate element standard solutions were prepared from concentrated (1,000 and 10,000 mg/L) stock solutions (Sigma-Aldrich TraceCERT) and acidified to pH=1.5.

2.3 Sample pre-treatment and analysis

One quarter of each aerosol-loaded filter was subjected to a microwave-assisted digestion in 30 mL tetrafluoromethoxyl vessels, which were then inserted into 100 mL tetrafluoromethoxyl vessels (vessel-inside-vessel technology (Nóbrega et al., 2015)). Stainless steel scissors were used for cutting the filters. According to the current legislation of the European Community in the field of air quality monitoring (UNI EN 14902:2005), the digestion mixture was composed of 2 mL HNO_3 and 0.5 mL H_2O_2; a mixture of 10 mL HPW and 1 mL H_2O_2 was introduced in the bigger vessel and the temperature was ramped to 220°C within 20 min, followed by a dwell time of other 20 min. Prior to the digestion, samples were left in contact with the digestion mixture for approximately 16 hours, in order to ensure the complete impregnation of the filter. The resulting solutions were filtered with Whatman Grade 5 cellulose filters, previously cleaned with 20 mL HPW, and then diluted to 15 ml with HPW. All the possible steps (filter cuts, digestion mixture preparation and filtration) were performed in a clean environment under a Class-100 laminar flow bench-hood. The reagent blanks, used for preparing the calibration standard solutions and for LOD calculation, were obtained by microwave-digesting the reagent mixture only. On the other hand, sample blanks were prepared similarly to the samples, by digesting some blank filters which had undergone the transport to and from Ny-Ålesund; sample blank concentrations were subtracted from sample concentrations, in order to eliminate the filter contribution. Sample blank concentrations (ppb or ppt) are reported in Table 3, together with the converted values in pg/m^3; the nominal air volume of 1152 m^3 and a solution volume of 15 mL were used for conversion.

Sets of instrumental blank and calibration checks were run at frequent intervals during the analysis sequence. The relative standard deviation for each element in each sample was always lower than 5%. The Certified Reference Material (CRM) NIST

1648a (“Urban Particulate Matter”) was used for verifying that a good recovery was obtained for each analyte before proceeding with sample analysis. The recovery rates of certified elements were higher than 80% for most of the analytes. Some of the typically geogenic analytes (i.e. Al and Ti) can be completely extracted only by using HF. Nevertheless, this is not a major problem since we mainly focussed on the variations of analyte concentrations throughout and among the investigated summer seasons.

Due to their very low concentrations, it was not possible to obtain reliable results for Tm and Lu. Therefore, these analytes were not included in data processing or graphical and statistical elaborations.

2.4 Enrichment factors

In order to estimate the influence of anthropogenic sources on the concentrations of major, minor and trace elements contained in PM_{10} samples, crustal and marine enrichment factors were calculated. Crustal Enrichment Factors (CEFs) were calculated with respect to the mean values for the Earth’s upper crust reported by Wedepohl (Wedepohl, 1995), in order to distinguish elements having geogenic or non-geogenic origin. The equation used is the following:

$$CEF_i = \frac{C_{i\ PM}/C_{r\ PM}}{C_{i\ crust}/C_{r\ crust}}$$

where $C_{i\ PM}/C_{r\ PM}$ and $C_{i\ crust}/C_{r\ crust}$ are the ratios between the concentration of the element i and the concentration of a reference element r in the sample and in the upper crust respectively; in this work, Al was selected as a reference element (Tahri et al., 2017). By convention, CEFs lower than 10 are taken as an indication that an element (called “not enriched”) has a prevailing geogenic origin, whereas CEFs between 10 and 100 indicate a moderate enrichment and CEFs higher than 100 indicate that the element (called “enriched”) has a prevailing non-geogenic origin (Lai et al., 2017; Tahri et al., 2017; Zajusz-Zubek et al., 2017). Similarly, Marine Enrichment Factors (MEFs) were calculated with respect to the mean abundances of elements in sea water reported by Goldberg (Goldberg, 1965), in order to distinguish elements having marine or non-marine origin; the abundance of In in sea water, not reported by Goldberg, was taken from Miyazaki (Miyazaki et al., 2008). The equation used is the following:

$$MEF_i = \frac{C_{i\,PM}/C_{r\,PM}}{C_{i\,sea}/C_{r\,sea}}$$

where $C_{i\ PM}/C_{r\ PM}$ and $C_{i\ sea}/C_{r\ sea}$ are the ratios between the concentration of the element *i* and the concentration of a reference element *r* in the sample and in sea water respectively; Na was selected as a reference element (Krnavek et al., 2012). Again, it was assumed that MEFs lower than 10 indicate an analyte not enriched with respect to sea water, whereas MEFs between 10 and 100 indicate a moderate enrichment and MEFs higher than 100 indicate that the analyte has a prevailing non-marine origin. The combination of both high CEFs and high MEFs allows the identification of elements probably having a strong anthropogenic contribution, as their main source is neither crustal nor marine.

2.5 Chemometric treatments and seasonal trends

Experimental results were processed by Lilliefors normality test, Kruskal-Wallis test, Principal Component Analysis (PCA) and Hierarchical Cluster Analysis (HCA) using XlStat 2017 software package, an add-on of Microsoft Excel. Information on the principles of these techniques can be found elsewhere (Einax et al., 1997; Massart et al., 1997; Ruxton and Beauchamp, 2008). The analytes whose concentrations were below the LOD in more than 30% of samples were not included in the treatments (Farnham et al., 2002). Conover-Iman test with a level of confidence of 95% was used for multiple pairwise comparison after the Kruskal-Wallis test. For performing PCA, values below the LOD were considered as equal to it and values below the sample blank were considered as equal to zero; the whole dataset was then autoscaled.

In order to gain a better comprehension of the temporal patterns shown by PCA and HCA and to study the behaviour of analytes which cannot be included in PCA (due to the absence of a sufficient amount of data above the LOD), the seasonal trends were evaluated. Metal concentrations were normalized by dividing them by the concentration of the same analyte in the first sampling of each campaign. In this way, the values reported for the first sampling are always equal to one, and the comparison of the temporal trends of metals having different concentration ranges are easier. Values below the LOD were reported in graph as equal to it.

2.6 HYSPLIT back-trajectories

Air mass back-trajectories were calculated using the NOAA HYSPLIT 4 transport model (Draxler and Rolph, 2003; Stein et al., 2015) and the GDAS meteorological data supplied by ARL (Air Resources Lab, http://ready.arl.noaa.gov). A propagation time of 120 h was set and Gruvebadet was used as the endpoint (78.92° N, 11.89°E, 0.0 m AGL); a new back-trajectory started every 6 hours.

3. Results and discussion

3.1 Elemental composition

The concentrations of major, minor and trace elements determined in the PM_{10} samples are shown in Supplementary Table 1 and 2; for converting the LOD from ppt (or ppb) to pg/m^3 (or fg/m^3), the actual solution volume and air volume of each sample were used. Table 4 reports the descriptive statistics for PM_{10} samples collected in Ny-Ålesund in 2010 (Bazzano et al., 2016a) and 2011-2013 (this study) campaigns: mean, median, minimum and maximum values, 5^{th} and 95^{th} percentile levels; for comparison, concentrations of major, minor and trace elements in PM_{10} samples collected in other parts of the world (Dai et al., 2016; Kulmatov and Hojamberdiev, 2010; Moreno et al., 2008b; Padoan et al., 2016; Toscano et al., 2005; Valdés et al., 2013) are reported. For calculating mean, median and percentiles, values below the LOD were considered as equal to it. Values below the sample blanks were not included in the calculations.

From Lilliefors normality test, it emerged that the results obtained for all analytes are not normally-distributed; therefore, non-parametric Kruskal-Wallis test and Conover-Iman pairwise comparison test were applied. Taking into account only samples collected in the period common to all the campaigns (May-July), the four campaigns were not significantly different for most of major and minor elements (Supplementary Table 3a). On the other hand, as regards As, Cd, Cu, Fe, Mo, Ti and most of lanthanides, data from one or two sampling campaigns do not belong to the same statistic population. For most of lanthanides, this is due to the samples collected in 2010 having higher concentrations, while for each of the other elements a different subdivision of sampling campaigns was found. In addition, it can be seen that 2012 and 2013 sampling campaigns presented a higher similarity among them than with the other two studied campaigns; this could be due to a higher similarity of the atmospheric conditions registered in these two years or to a change in the mid-latitudes emissions due to the introduction of some new emission regulations. The same tests were used for checking the presence of significant differences among samples collected in spring and summer (Supplementary Table 3b). Again, no significant differences were found for most of the elements, except for Al, Ca, Cd, Cu, Mn, Pb and V: the latter presented significantly higher concentrations in summer than in spring, while for the other analytes it is the opposite. Although for Al, Ca and Mn this variability is likely due to natural phenomena, it is possible that the seasonal variability of Cd, Cu, Pb and V is due to anthropogenic activities, as demonstrated for Pb by isotopic analysis (Bazzano et al., 2016b).

3.2 Ce-La-V ternary diagram

For a first identification of the sources of V, a Ce-La-V ternary diagram was used (Becagli et al., 2017; Moreno et al., 2008a; Moreno et al., 2008b). For building this graph, the concentration of Ce and La were multiplied by an adequate coefficient (1.54 and 3.1 respectively) so that the centre of the diagram represents the composition of the upper crust (Henderson and Henderson, 2009). In this way, PM samples which are strongly influenced by refinery emissions are generally located near to the lower left corner of the diagram (Moreno et al., 2008a; Moreno et al., 2008b), while PM samples which are strongly influenced by ship emissions or other oil combustion processes are generally located near to the lower right corner (Becagli et al., 2017; Moreno et al., 2008a; Moreno et al., 2008b); in addition, Moreno et al. suggested that PM samples strongly influenced by vehicular traffic emissions are likely located close to the triangle centre, slightly toward Ce due to the abrasive loss of Ce-rich PM from catalytic converters (Moreno et al., 2008b). Figure 2 shows the Ce-La-V ternary diagram for PM_{10} samples collected near to Ny-Ålesund during 2010-2013 sampling campaigns.

Samples are mainly located in an area ranging from the lower right corner to the centre of the diagram, therefore the two most important sources of V are likely weathering of the upper crust and ship emissions; a contribution of refinery emissions can be excluded, while a contribution of vehicular emissions is conceivable only for very few samples collected in summer 2012. In particular, three samples collected in July, August and September 2012 are located in the upper right part of the diagram, due to their anomalously high content of Ce and, to a lesser extent, V; as a consequence, a possible contribution from vehicle exhaust emissions cannot be excluded for these samples. As it regards the seasonal distribution of samples in the diagram, it is possible to see that samples strongly influenced by crustal sources were mainly collected in April; considering that, in spring, the soil of Svalbard Islands is generally still covered by snow and ice, this fact can be explained by the presence of PM deriving from mid-latitudes (Arctic haze) (Yli-Tuomi et al., 2003). On the other hand, samples strongly influenced by oil combustion were mainly collected in June and July, period during which the marine traffic in the fjord is generally high, due to the reopening of research bases and to the presence of cruise ships.

3.3 Enrichment factors

Figure 3 reports the box plots for all the calculated EFs. From CEFs and MEFs, it emerged that the origin of Ba, Co, Fe, Mn, Ti, V and lanthanides in the analysed samples is mostly geogenic, the origin of Ca and Mg is primarily marine and the origin of As, Cd, Cu, In, Mo, Ni, Pb and Zn is mainly anthropogenic. Nevertheless, some of these elements seem to have a mixed origin, or a different origin in some of the analysed samples; in particular, the concentrations of Ca, In, Ni, Pb and Zn seem to derive, in some of the samples, from a crustal source, and the concentrations of Co and V might depend, in some samples, on anthropogenic sources. As regards K, both CEFs and MEFs are generally lower than 10, indicating that its concentration is likely influenced by both marine and crustal sources, while an anthropogenic contribution might be excluded. The calculation of EFs is a useful way for obtaining a first estimate of the different sources of the analytes in PM samples; nevertheless, due to the simplicity of the calculation and to the assumptions made in the interpretation of results, the information obtained should be confirmed by other approaches, e.g. the study of the analyte temporal variations and multivariate analysis.

3.4 Chemometric treatments and seasonal trends

The complexity of the matrices and of the phenomena under study renders interpretation of experimental results difficult. PCA and HCA can be a valuable tool for this aim, owing to their multivariate approach, which takes into account the behaviour of multiple variables simultaneously (Einax et al., 1997; Massart et al., 1997). With the aid of PCA and HCA it was possible to obtain a global graphical representation of data and to investigate relationships among variables, similarities and differences among sampling periods, and to identify the causes of the behaviour of the investigated analytes (e.g. the element sources). In the following treatments, the names used for the samples correspond to the beginning of the sampling.

3.4.1 2012 campaign

For having information on the seasonal variability of PM_{10} composition, we performed PCA including data from one sampling campaign at a time. The sampling campaign carried out in 2012, which is the longest of the three campaigns presented in this study, is the one in which the seasonal variability of PM_{10} is more visible. Therefore, it is the only single-campaign PCA reported. Score and loading plots obtained by PCA for 2012 samples are shown in Figure 4 (PC1vs. PC2). The first PC, retaining 57.9% of the total variance of the dataset, is mainly associated with analytes having a geogenic origin, such as Al, Ba, Fe, Mn, Ti and lanthanides, except Ce (the label “REEs” in the loading plot cumulatively indicates all lanthanides except the latter). By looking at the score plot, it is possible to distinguish samples collected in April and May, having positive scores on PC1, from samples collected in June, August and September, having negative scores (except 12 Jun); samples collected in July, though, are spread among the two groups. Considering that, in spring, the soil of Svalbard Islands is still covered by snow and ice, it is likely that long-range transport of PM from mid-latitudes took place in this period, thus influencing the composition of PM_{10} samples collected near to Ny-Ålesund; this result is coherent with previous findings, evidencing the so-called “Arctic haze” in spring (Lupi et al., 2016; Udisti et al., 2016). A further proof of the different sources of the PM_{10} collected in the two seasons can be found in Figure 5, showing HYSPLIT back-trajectories calculated for two samples: 15 May (positive scores on PC1) and 3 Aug (negative scores on PC1). The latter is characterized by a low variability in the direction of the back-trajectories and by a path that remains within the Arctic circle; on the other hand, some of the back-trajectories calculated for the sample collected in spring indicate a mid-latitude provenance, ranging from Europe to eastern Asia. The fact that some samples collected in July present positive scores on PC1, which means that the concentrations of geogenic analytes in those samples were relatively high, can be explained considering the unusual atmospheric conditions registered in that period; in fact, as shown by HYSPLIT back-trajectories reported in Moroni et al. (2016), air currents coming from eastern Russia arrived in Ny-Ålesund, therefore a PM contribution deriving from Gobi Desert cannot be excluded (Huang et al., 2015). The position of Ce with respect to the other lanthanides suggests that this element might have a non-geogenic, i.e. anthropogenic, origin. This hypothesis is supported by the evidence that, for five samples collected in 2012, the calculated CEFs for Ce are higher than 10.

PC2, retaining 14.1% of the total variance, is associated with the marine aerosol source, as Mg and Na present the highest loadings. Other analytes having high loadings on PC2 are K, and, to a lesser extent, Ca, Mo and Ni; while Ca, K, Mg and Na are most likely to have a natural origin, this is not true for the other two analytes, as indicated by their MEFs. For Ni, airborne pollution deriving from ship emissions might be the main source during spring, when the air masses coming from mid-latitudes overpass the ocean and become enriched of analytes from marine aerosol. No clear subdivision of samples according to PC2 can be seen.

Figure 6 shows the dendrogram obtained by Q-mode HCA, where three main clusters of analytes can be seen. The first cluster is composed by analytes having high loadings on PC1 (i.e. Al, Ba, Fe, Mn, Ti and lanthanides), which are typically geogenic; as expected, at a lower level of dissimilarity it is possible to see that lanthanides form a distinct cluster from the other five analytes. The second cluster is composed by analytes probably having an anthropogenic origin, i.e. As, Cd, Ce, Cu and Zn; at a lower level of dissimilarity, it is possible to distinguish a small cluster composed of As and Cd, a small cluster composed of Cu and Zn, and Ce as an outlier. As and Cd are commonly emitted during combustion and industrial production processes (Pacyna et al., 2007; Ragazzi, 2017), which are likely occurring at mid-latitudes; Cu and Zn are likely associated with non-exhaust vehicle emissions, as these elements are common indicators of brake and tyre wear (Birmili et al., 2006; Councell et al., 2004; Fauser et al., 1999; Lough et al., 2005); considering its position in the dendrogram, Ce might also derive from vehicular emissions, as this element is often used in catalytic converters (Angelidis and

Sklavounos, 1995; Arul Mozhi Selvan et al., 2014; Moreno et al., 2008b; Sajeevan and Sajith, 2016; Silveston, 1995). The third cluster is composed by analytes deriving from marine aerosol: apart from K, Mg and Na, it is possible to identify a small cluster composed of Ca and Mo, which can partially have a crustal contribution, and a small cluster composed of Co, Ni and V; therefore, airborne pollution deriving from ship emissions might be the main source not only for Ni but also for Co and V, even though some other individual sources might be present for these analytes. Similar information was obtained by PCA, by investigating PC3 and PC4 (Supplementary Figure 1): despite the low portion of the total variance retained by these PCs, they carry information on PM sources contributing only slightly to the overall PM composition (i.e. anthropogenic sources of PM collected in a pristine environment). In particular, it is evident that the three samples having the highest concentration of Co, Ni and V have been collected at the end of July, when at least two cruise ships having more than 1500 passengers travelled in Kongsfjorden Bay (Zhan et al., 2014).

For making hypothesis on the possible sources of Pb, a probably anthropogenic analyte which could not be included in PCA and HCA, its seasonal trend was used. Figure 7 shows that the seasonal trend registered for Pb is analogous to the one obtained for As, Cd and Zn, which presented relatively high concentrations in samples collected in April and in the first part of May, when long-range transport processes from mid-latitudes take place. Therefore, it is likely that the spring origin of Pb coincides with the one of the other analytes, i.e. anthropogenic continental sources such as vehicular traffic, incinerators or industries. Isotopic analysis indicated that mining and smelting activities in the Rudny Altay region (Central Eurasia) were the main sources of atmospheric lead in spring, whereas industrial emission in north-eastern North America, were the main sources of atmospheric lead in summer (Bazzano et al., 2016b). Zn presents some concentration peaks in June and July and a sharp increase at the beginning of September, not coinciding with the trends registered for As, Cd and Pb; therefore, a second source for Zn might have been introduced from the beginning of June, explaining its different seasonal trend. The other possible source for this element can be non-exhaust vehicle emissions, fact confirmed by the similarity between Cu and Zn shown by HCA (Figure 6, Paragraph 3.3.1). In fact, it is likely that the local vehicle contribution became higher in summer, when the population of Ny-Ålesund is greater and the long-range transport processes of PM from mid-latitudes are lower.

3.4.2 Comprehensive treatment (2010-2013)

A comprehensive PCA including data from the four successive sampling campaigns (2010-2013) was executed. The first PC (46.8% of variance, not shown) is associated with the content of crustal elements, as Al, Ba, Fe, Mn and lanthanides (cumulatively indicated in the graph as "REEs") present the highest loadings; two samples collected in July 2013 present by far the highest scores on this PC. The score and loading plot for PC2 vs. PC3 (10.8% and 7.6% of variance respectively) are reported in Figure 8. Two main groups of analytes can be identified in the loading plot: As, Cd, Pb and Zn, generally representing anthropogenic contributions, and Mg and Na, representing the marine spray input; a cluster made of Co, Ni and V, having small positive loadings, lays in the middle of the two main clusters and might be attributed to ship emissions. Ca and K lay in the same direction as Mg and Na, but their loadings on PC3 are much smaller; considering that they presented quite high loadings on PC1 (not shown), it is possible to hypothesize a mixed crustal-marine origin for these elements. Two samples collected in April 2010 and one sample collected in July 2013 have the highest scores on PC2, as a consequence of their relatively high content of the analytes constituting the first cluster; for 2010 samples, this can be attributed to the several eruptions of the Icelandic Eyjafjöll Volcano which took place in that spring. The score plot of Figure 8a shows that samples located at positive values of PC2, having therefore relatively high concentrations of marine and anthropogenic analytes, were prevalently collected in spring. Apart from a slight prevalence of samples collected in 2010 in the lower right portion of the graph (positive values of PC2 and negative values of PC3), which may still be attributed to the Eyjafjöll eruptions, no clear subdivision of samples according to the sampling campaign can be seen on either PC1, PC2 or PC3; consequently, it is possible to state that neither the natural (crustal and marine) nor the anthropogenic contribution significantly changed during the investigated period. This result is a confirmation of what emerged from Kruskal-Wallis and Conover-Iman tests.

3.5 Rare Earth Element patterns

As mentioned in paragraph 3.1, REE concentrations determined in the PM_{10} samples are shown in Supplementary Table 2 and their descriptive statistics are reported in

Table 4; values below the LOD were not included in any of the following calculations. The overall shape of the lanthanides concentration pattern is the naturally occurring saw-tooth distribution, i.e. the odd-even pattern following the Oddo-Harkins rule (Henderson, 1984; Piper and Bau, 2012; Schmidt et al., 1963); Figure 9a shows the mean lanthanide concentrations found for each sampling campaign. Figure 9b shows, for each sampling campaign, the mean lanthanide concentrations normalized to the average shale reported by Byrne and Sholkovitz (Byrne and Sholkovitz, 1996), while Figure 9c reports the mean normalized lanthanide concentrations for each month of 2012 sampling campaign. It is generally agreed that the average shale REEs pattern represents that of the upper crust (Taylor and McLennan, 1985); therefore, normalization to the average shale allows the removal of the systematic differences existing between adjacent elements and to highlight significant composition differences arising from the parent material. In this case, the exact value of the normalized concentration has no meaning, hence only the shape of the pattern and the relative values should be taken into account. For each sample, the pattern has a slightly negative slope, indicating a small light REEs enrichment; in fact, the calculated Pr/Yb ratios (Figure 9d) are usually greater than one (Lawrence et al., 2006). A light REEs enrichment is generally a consequence of weathering of rocks with unstable mineralogy under surface conditions, such as ultramafic and basaltic rocks (Taylor and McLennan, 1985). The mean patterns registered for the investigated campaigns and the mean patterns registered for each month of 2012 sampling campaign are approximately the same, indicating that, in the investigated period, the sources of geogenic analytes in the PM_{10} collected near to Ny-Ålesund do not vary significantly.

Ce anomaly was calculated as follows:

$$Ce_{anom.} = \frac{Ce_N}{\sqrt{La_N \cdot Pr_N}}$$

where the subscript "N" indicates that the concentrations are normalized to the average shale. Ce anomaly represents the deviation of Ce concentration from that expected by calculating the geometric average of the concentrations of La and Pr in shale; a deviation from unity of this value is thus a measure of the deviation (fractionation) of Ce from the expected REEs behaviour (Bazzano et al., 2016a; Giardi et al., 2018; Taylor and McLennan, 1985). Ce anomaly in PM samples can arise from an anthropogenic release of Ce in the atmosphere or from the geochemical characteristics of the parent rock, in their turn deriving from the redox conditions registered during the rock formation: under alkaline conditions, Ce^{3+} can be oxidized by atmospheric oxygen to Ce^{4+}, and the formation of the insoluble CeO_2 modifies the distribution of this element in the environment (De Baar et al., 1988; Henderson, 1984). Figure 9e shows Ce anomaly for each month of each sampling campaign: its value was higher than 1 in most cases. In particular, high Ce enrichments were registered in August 2012 and 2013 and in September 2012; considering that, in these months, the input of PM from mid-latitudes was negligible, the high Ce concentrations can be attributed to local pollution. The observation of Figure 2 and 6 (Paragraph 3.2 and 3.4.1) drove to the same conclusion.

Analogously to Ce, Eu anomaly was calculated as follows:

$$Eu_{anom.} = \frac{Eu_N}{\sqrt{Sm_N \cdot Gd_N}}$$

Eu anomaly always reflects the geochemical characteristics of the parent rock, as the additional oxidation state of this element allows the substitution of Eu^{2+} in place of Ca^{2+}, Pb^{2+} or Sr^{2+} in some minerals, particularly in feldspars, determining an Eu enrichment with respect to the other REEs; as a consequence, most of the other minerals (both igneous and sedimentary) commonly present a complementary Eu depletion with respect to the other REEs. Figure 9f shows Eu anomaly for each month of each sampling campaign. Eu anomaly was higher than 1 in most cases, suggesting that the geogenic portion of collected PM_{10} mostly derives from weathering of feldspars. Nevertheless, no specific trends were registered for Eu anomaly; Eu depletion with respect to other REEs was only registered in samples collected in March and April 2011 and in May 2013, probably indicating a prevalence of different geogenic sources for the PM_{10} collected during those months.

3.6 Comparison with other sites

For comparison, concentrations of major, minor and trace elements in PM_{10} samples collected in other parts of the world (Kulmatov and Hojamberdiev, 2010; Marx et al., 2014; Moreno et al., 2008b; Öztürk et al., 2012; Padoan et al., 2016; Toscano et al., 2005; Truzzi et al., 2017) are reported in Table 4. As expected, metal concentrations found in PM_{10} samples collected in Terra Nova Bay (Antarctica) are comparable with the ones of Ny-Ålesund, for all the investigated elements. The other areas presented for comparison generally show remarkably higher element concentrations than the median values of this study: this can be explained considering that the atmospheric circulation causes even remote areas located at mid-latitudes (e.g. Abramov Glacier and New Zealand's Southern Alps) to be affected by continental emissions. Nevertheless, the concentration of anthropogenic analytes registered in samples collected in New Zealand's Southern Alps are comparable with the 95th percentile of the results obtained in this study, which might be considered representative of concentrations registered in spring.

Very few studies have been executed on the REEs content in PM_{10} samples, and most of them regard PM_{10} samples collected near mines, not directly comparable with our study results. Comparison data reported for REEs in Table 4b derive from PM_{10} samples collected in remote and rural areas. The results presented for comparison are remarkably higher; this fact can be attributed to the permanence, in Svalbard Islands, of a snow and ice cover for most of the year, causing weathering phenomena to be markedly reduced with respect to other parts of the world.

4. Conclusions

In this study, the elemental composition of PM_{10} samples collected near to Ny-Ålesund (Norwegian Arctic) in the sampling campaigns 2011-2013 was investigated, and compared with results obtained for 2010 sampling campaign, previously published. Natural (crustal and marine) and anthropogenic Arctic PM sources were identified, and a better understanding of the effects of short- and long-range transport processes taking place in this remote area was made possible; these data can be useful for studies on the effect of Arctic PM on the climate change, as well as for a comparison of the composition of PM_{10} collected in other remote and anthropized areas.

Crustal Enrichment Factors and Marine Enrichment Factors allowed us the identification of elements having geogenic, marine or other origin. PCA and HCA allowed us a better understanding of the sources of different elements and to lay the basis for an interpretation of the chemical and physical processes concerning the Arctic atmosphere; seasonal concentration trends were helpful for the source identification of analytes which could not be included in the chemometric treatments. Airborne pollution deriving from ship fuels, local vehicle (non-exhaust) and continental emissions (e.g. incinerators or industries) were the main sources of anthropogenic elements. Most of the elements determined in PM_{10} samples collected near to Ny-Ålesund present seasonal variations:

for both geogenic and anthropogenic elements, concentrations are generally higher in spring, when the ground is almost entirely covered by snow and ice, suggesting that long-range transport processes of PM from mid-latitudes might be taking place; on the other hand, the concentrations of anthropogenic metals related to ship emissions (i.e. Co, Ni and V), peak in late spring and summer, when the marine traffic in the fjord is generally high due to the reopening of research bases and to the presence of several cruise ships in Kongsfjorden Bay. For most of the analytes, the four sampling campaigns were not significantly different; therefore, in the studied period, the composition of PM_{10} in Ny-Ålesund did not vary remarkably. For all the investigated elements, concentration values registered in PM_{10} samples collected in Terra Nova Bay (Antarctica) are comparable with the ones of this study; all the other areas considered for comparison exhibit remarkably higher element concentrations.

5. Acknowledgments

This study was partially funded by the Italian Ministry of Education, University and Research (PRIN n° 20092C7KRC_002). The logistic assistance of the Polar Support Unit of the National Research Council (Department of Earth and Environment) is gratefully acknowledged.

6. References

Angelidis TN, Sklavounos SA. A SEM-EDS study of new and used automotive catalysts. Applied Catalysis A: General 1995; 133: 121-132.

Arul Mozhi Selvan V, Anand RB, Udayakumar M. Effect of Cerium Oxide Nanoparticles and Carbon Nanotubes as fuel-borne additives in Diesterol blends on the performance, combustion and emission characteristics of a variable compression ratio engine. Fuel 2014; 130: 160-167.

Barrie LA, Gregor D, Hargrave B, Lake R, Muir D, Shearer R, et al. Arctic contaminants: sources, occurrence and pathways. Science of the Total Environment 1992; 122: 1-74.

Barrie LA, Hoff RM. Five years of air chemistry observations in the Canadian Arctic. Atmospheric Environment 1985; 19: 1995-2010.

Bazzano A, Ardini F, Becagli S, Traversi R, Udisti R, Cappelletti D, et al. Source assessment of atmospheric lead measured at Ny-Ålesund, Svalbard. Atmospheric Environment 2015; 113: 20-26.

Bazzano A, Ardini F, Grotti M, Malandrino M, Giacomino A, Abollino O, et al. Elemental and lead isotopic composition of atmospheric particulate measured in the Arctic region (Ny-Ålesund, Svalbard Islands). Rend. Fis. Acc. Lincei 2016a; 27: S73-S84.

Bazzano A, Cappelletti D, Udisti R, Grotti M. Long-range transport of atmospheric lead reaching Ny-Ålesund: inter-annual and seasonal variations of potential source areas. Atmospheric Environment 2016b; 139.

Becagli S, Anello F, Bommarito C, Cassola F, Calzolai G, Di Iorio T, et al. Constraining the ship contribution to the aerosol of the central Mediterranean. Atmospheric Chemistry and Physics 2017; 17: 2067-2084.

Birmili W, Allen AG, Bary F, Harrison RM. Trace metal concentrations and water solubility in size-fractionated atmospheric particles and influence of road traffic. Environ. Sci. Technol. 2006; 40: 1144-1153.

Bodhaine BA, Dutton EG, DeLuisi JJ, Herbert GA, Shaw GE, Hansen ADA. Surface aerosol measurements at Barrow during AGASP-II. Journal of Atmospheric Chemistry 1989; 9: 213-224.

Byrne RH, Sholkovitz ER. Marine chemistry and geochemistry of the lanthanides. In: Gschneider KAJ, Eyring LR, editors. Handbook on the Physics and Chemistry of the Rare Earths. 23. Elsevier, 1996, pp. 497-593.

Cappelletti D, Azzolini R, Langone L, Ventura S, Viola A, Aliani S, et al. Environmental changes in the Arctic: an Italian perspective. Rend. Fis. Acc. Lincei 2016; 27: S1-S6.

Clarke AD. In-situ measurements of the aerosol size distributions, physicochemistry and light absorption properties of Arctic haze. Journal of Atmospheric Chemistry 1989; 9: 255-266.

Councell TB, Duckenfield KU, Landa ER, Callender E. Tire-wear particles as a source of zinc to the environment. Environ. Sci. Technol. 2004; 38: 4206-4214.

Dai Q, Li L, Li T, Bi X, Zhang Y, Wu J, et al. Atmospheric Signature and Potential Sources of Rare Earth Elements in Size-Resolved Particulate Matter in a Megacity of China. Aerosol and Air Quality Research 2016; 16: 2085-2095.

De Baar HJW, German CR, Elderfield H, Van Gaans P. Rare earth element distribution in anoxic waters of the Cariaco Trench. Geochimica et Cosmochimica Acta 1988; 52: 1203-1219.

Draxler RR, Rolph GD. HYSPLIT (HYbrid single-particle Lagrangian integrated trajectory) model access via NOAA ARL READY. NOAA Air Resources Laboratory, Silver Spring, MD. Dostupno na: http://ready. arl. noaa. gov/HYSPLIT. php (06. 06. 2010.) 2003.

Einax W, Zwanziger HW, Gei S. Chemometrics in environmental analysis. Weinhem, Germany: Wiley-VHC, 1997.

Farnham IM, Singh AK, Stetzenbach KJ, K.H. J. Treatment of nondetects in multivariate analysis of groundwater geochemistry data. Chemometrics and Intelligent Laboratory Systems 2002; 60: 265-281.

Fauser P, Tjell JC, Mosbaek H, Pilegaard K. Quantification of tire-tread particles using extractable organic zinc as tracer. Rubber chemistry and technology 1999; 72: 969-977.

Giardi F, Becagli S, Traversi R, Frosini D, Severi M, Caiazzo L, et al. Size distribution and ion composition of aerosol collected at Ny-Ålesund in the spring-summer field campaign 2013. Rend. Fis. Acc. Lincei 2016; 27: S47-S58.

Giardi F, Traversi R, Becagli S, Severi M, Caiazzo L, Ancillotti C, et al. Determination of Rare Earth Elements in multi-year high-resolution Arctic aerosol record by double focusing Inductively Coupled Plasma Mass Spectrometry with desolvation nebulizer inlet system. Sci Total Environ 2018; 613-614: 1284-1294.

Goldberg ED. Chapter 5: Minor elements in sea water. In: Riley JP, Skirrow G, editors. Chemical Oceanography. Academic Press, London (UK), 1965, pp. 163-196.

Gong SL, Barrie LA. Trends of heavy metal components in the Arctic aerosols and their relationship to the emissions in the Northern Hemisphere. Sci Total Environ 2005; 342: 175-183.

Henderson P. Rare Earth Element Geochemistry. New York: Elsevier, 1984.

Henderson P, Henderson GM. The Cambridge Handbook of Earth Science Data. Cambridge: University Press, 2009.

Huang Z, Huang J, Hayasaka T, Wang S, Zhou T, Jin H. Short-cut transport path for Asian dust directly to the Arctic: a case study. Environmental Research Letters 2015; 10: 114018.

Krnavek L, Simpson WR, Carlson D, Domine F, Douglas TA, Sturm M. The chemical composition of surface snow in the Arctic: Examining marine, terrestrial, and atmospheric influences. Atmospheric Environment 2012; 50: 349-359.

Kulmatov R, Hojamberdiev M. Distribution of heavy metals in atmospheric air of the arid zones in Central Asia. Air Quality, Atmosphere & Health 2010; 3: 183-194.

Lai AM, Shafer MM, Dibb JE, Polashenski CM, Schauer JJ. Elements and inorganic ions as source tracers in recent Greenland snow. Atmospheric Environment 2017; 164: 205-215.

Lawrence MG, Greig A, Collerson KD, Kamber BS. Rare Earth Element and Yttrium Variability in South East Queensland Waterways. Aquatic Geochemistry 2006; 12: 39-72.

Leck C, Persson C. Seasonal and short–term variability in dimethylsulfide, sulfur dioxide and biogenic sulfur and sea salt aerosol particles in the arctic marine boundary layer during summer and autumn. . Tellus Series B–Chemical and Physical Meteorology 1996; 48: 272-299.

Lough GC, Schauer JJ, Park JS, Shafer MM, Deminter JT, Weinstein JP. Emissions of metals associated with motor vehicle roadways. Environ. Sci. Technol. 2005; 39: 826-836.

Lupi A, Busetto M, Becagli S, Giardi F, Lanconelli C, Mazzola M, et al. Multi-seasonal ultrafine aerosol particle number concentration measurements at the Gruvebadet observatory, Ny-Ålesund, Svalbard Islands. Rend. Fis. Acc. Lincei 2016; 27: S59-S71.

Marx SK, Lavin KS, Hageman KJ, Kamber BS, O'Loingsigh T, McTainsh GH. Trace elements and metal pollution in aerosols at an alpine site, New Zealand: Sources, concentrations and implications. Atmospheric Environment 2014; 82: 206-217.

Massart DL, Vandenginste BGM, Buydens LMC, De Jono S, Leqi PJ, Smeyers-Verbeke J. Handbook of chemometrics and qualimetrics, Parts A and B. Amsterdam: Elsevier, 1997.

Mazzola M, Viola AP, Lanconelli C, Vitale V. Atmospheric observations at the Amundsen-Nobile Climate Change Tower in Ny-Ålesund, Svalbard. Rend. Fis. Acc. Lincei 2016; 27: S7-S18.

Minguillón MC, Querol X, Baltensperger U, Prévôt ASH. Fine and coarse PM composition and sources in rural and urban sites in Switzerland: local or regional pollution? Sci Total Environ 2012; 427-428: 191-202.

Miyazaki A, Kimura A, Tao H. Determination of indium in sea water around Japan and in the Pacific Ocean by ICP-MS after preconcentration using Chelex-100 chelating resin. Bunseki Kagaku 2008; 57: 555-561.

Moreno T, Querol X, Alastuey A, Gibbons W. Identification of FCC refinery atmospheric pollution events using lanthanoid- and vanadium-bearing aerosols. Atmospheric Environment 2008a; 42: 7851-7861.

Moreno T, Querol X, Alastuey A, Pey J, Minguillón MC, Pérez N, et al. Lanthanoid geochemistry of urban atmospheric particulate matter. Environ. Sci. Technol. 2008b; 42: 6502-6507.

Moroni B, Cappelletti D, Ferrero L, Crocchianti S, Busetto M, Mazzola M, et al. Local vs long-range sources of aerosol particles upon Ny-Ålesund (Svalbard Islands): mineral chemistry and geochemical records. Rend. Fis. Acc. Lincei 2016; 27: S115-S127.

Nóbrega JA, Pirola C, Richter RC. Think blank. Clean chemistry tools for atomic spectroscopy: Ikonos, 2015.

Öztürk F, Zararsız A, Dutkiewicz VA, Husain L, Hopke PK, Tuncel G. Temporal variations and sources of Eastern Mediterranean aerosols based on a 9-year observation. Atmospheric Environment 2012; 61: 463-475.

Pacyna EG, Pacyna JM, Fudala J, Strzelecka-Jastrzab E, Hlawiczka S, Panasiuk D, et al. Current and future emissions of selected heavy metals to the atmosphere from anthropogenic sources in Europe. Atmospheric Environment 2007; 41: 8557-8566.

Padoan E, Malandrino M, Giacomino A, Grosa MM, Lollobrigida F, Martini S, et al. Spatial distribution and potential sources of trace elements in PM10 monitored in urban and rural sites of Piedmont Region. Chemosphere 2016; 145: 495-507.

Piper DZ, Bau M. Normalized Rare Earth Elements in Water, Sediments, and Wine: Identifying Sources and Environmental Redox Conditions. American Journal of Analytical Chemistry 2012; 4: 69-83.

Polissar AV, Hopke PK. Atmospheric aerosol over Alaska 2. Elemental composition and sources. Journal of Geophysical Research 1998; 103: 19045-19057.

Quinn PK, Shaw GE, Andrews E, Dutton EG, Ruoho-Airola T, Gong SL. Arctic haze: current trends and knowledge gaps. Tellus B: Chemical and Physical Meteorology 2007; 59B: 99-114.

Ragazzi M. Pollution and the atmosphere: designs for reduced emissions. CRC Press, 2017.

Ruxton GD, Beauchamp G. Some suggestions about appropriate use of the Kruskal–Wallis test. Animal Behaviour 2008; 76: 1083-1087.

Sajeevan AC, Sajith V. Synthesis of stable cerium zirconium oxide nanoparticle – Diesel suspension and investigation of its effects on diesel properties and smoke. Fuel 2016; 183: 155-163.

Schmidt RA, Smith RH, Lasch JE, Mosen AW, Olehy DA, Vasilevshis J. Abundances of fourteen Rare-Earth Elements, Scandium and Yttrium in Meteoritic and Terrigenous Matter. Geochimica et Cosmochimica Acta 1963; 27: 577-622.

Shaw GE. Evidence for a central Eurasian source area of Arctic haze in Alaska. Nature 1982; 299: 815-818.

Silveston PL. Automotive exhaust catalysis under periodic operation. Catalysis today 1995; 25: 175-195.

Stein AF, Draxler RR, Rolph GD, Stunder BJB, Cohen MD, Ngan F. NOAA's HYSPLIT Atmospheric Transport and Dispersion Modeling System. Bulletin of the American Meteorological Society 2015; 96: 2059-2077.

Tahri M, Benchrif A, Bounakhla M, Benyaich F, Noack Y. Seasonal variation and risk assessment of PM2.5 and PM2.5-10 in the ambient air of Kenitra, Morocco. Environ Sci Process Impacts 2017; 19: 1427-1436.

Talbi A, Kerchich Y, Kerbachi R, Boughedaoui M. Assessment of annual air pollution levels with PM1, PM2.5, PM10 and associated heavy metals in Algiers, Algeria. Environ Pollut 2018; 232: 252-263.

Taylor SR, McLennan SM. The continental crust: its composition and evolution. Oxford (UK): Blackwell Scientific Publications, 1985.

Toscano G, Gambaro A, Moret I, Capodaglio G, Turetta C, Cescon P. Trace metals in aerosol at Terra Nova Bay, Antarctica. J Environ Monit 2005; 7: 1275-80.

Truzzi C, Annibaldi A, Illuminati S, Mantini C, Scarponi G. Chemical fractionation by sequential extraction of Cd, Pb, and Cu in Antarctic atmospheric particulate for the characterization of aerosol composition, sources, and summer evolution at Terra Nova Bay, Victoria Land. Air Quality, Atmosphere & Health 2017; 10: 783-798.

Udisti R, Bazzano A, Becagli S, Bolzacchini E, Caiazzo L, Cappelletti D, et al. Sulfate source apportionment in the Ny-Ålesund (Svalbard Islands) Arctic aerosol. Rend. Fis. Acc. Lincei 2016; 27: S85-S94.

Valdés A, Polvé M, Munoz M, Toutain JP, Morata D. Geochemical features of aerosols in Santiago de Chile from time series analysis. Environmental Earth Sciences 2013; 69: 2073-2090.

Wedepohl KH. The composition of the continental crust. Geochimica et Cosmochimica Acta 1995; 59: 1217-1232.

Yli-Tuomi T, Venditte L, Hopke PK, Basunia MS, Landsberger S, Viisanen Y, et al. Composition of the Finnish Arctic aerosol: collection and analysis of historic filter samples. Atmospheric Environment 2003; 37: 2355-2364.

Zajusz-Zubek E, Radko T, Mainka A. Fractionation of trace elements and human health risk of submicron particulate matter (PM1) collected in the surroundings of coking plants. Environ Monit Assess 2017; 189: 389.

Zhan J, Gao Y, Li W, Chen L, Lin H, Lin Q. Effects of ship emissions on summertime aerosols at Ny–Ålesund in the Arctic. Atmospheric Pollution Research 2014; 5: 500-510.

Table 1. Sampling dates and number of samples collected in each campaign.

Campaign	Start date	End date	Samples
2010	16th March	16th September	36
2011	29th March	26th July	24
2012	17th April	7th September	36
2013	1st May	13th September	33

2010 campaign results are reported in Bazzano et al., 2016a.

Table 2. Model and features of the instrumental techniques used for the analysis.

Technique	Model	Features	Analytes
ICP-OES	Perkin Elmer Optima 7000 DV	Mira Mist nebulizer, cyclonic spray chamber, dual Échelle monochromator, dual CCD detector	Na, Mg, K, Ca
HR-ICP-MS	Thermo Finnigan Element 2	Conikal nebulizer, Scott spray chamber, magnetic and electric sector, SEM detector	Al, As, Ba, Cd, Ce, Co, Cu, Dy, Er, Eu, Fe, Gd, Ho, In, La, Lu, Mn, Mo, Nd, Ni, Pb, Pr, Sm, Tb, Ti, Tm, V, Yb, Zn

Table 3. Experimental conditions and limits of detection (LOD) of the analytes of interest with the technique used for their determination.

	HR-ICP-MS														
	Al	**As**	**Ba**	**Cd**	**Co**	**Cu**	**Fe**	**In**	**Mn**	**Mo**	**Ni**	**Pb**	**Ti**	**V**	**Zn**
Isotope **resolution**	27 LR-MR	75 MR	135-137 LR-MR	111-112-114 LR	59 LR-MR	63-65 LR-MR	56-57 MR	115 MR	55 LR-MR	95-98 LR-MR	60-61-62 LR-MR	206-207-208 LR-MR	46-47-48 LR-MR	51 LR-MR	66-68 LR-MR
LOD (ppt)	400	42	62	2.3	1.9	11	400	1.8	8.6	4.2	45	40	750	58	190
LOD (fg/m^3)	5200	550	810	30	25	140	5200	23	110	55	590	520	9800	760	2500
Sample blank (ppb)	0.63	< LOD	1.1	< LOD	< LOD	< LOD	3.2	< LOD	0.040	0.019	0.50	0.23	< LOD	< LOD	4.5
Sample blank (pg/m^3)	8.2	< LOD	14	< LOD	< LOD	< LOD	42	< LOD	0.52	0.25	6.5	3.0	< LOD	< LOD	59

	HR-ICP-MS															ICP-OES			
	7. **La**	8. **Ce**	**Pr**	**Nd**	**Sm**	**Eu**	**Gd**	**Tb**	**Dy**	**Ho**	**Er**	**Tm**	**Yb**	**Lu**		**Ca**	**K**	**Mg**	**Na**
Isotope **resolution**	139 LR	140 LR	141 LR	143-146 LR	147-149 LR	151-153 LR	155-157 LR	159 LR	161-163 LR	165 LR	166-167 LR	169 LR	172 LR	175 LR	**Wavelength (nm)**	317.9	769.9	285.2	589.6
LOD (ppt)	0.92	2.5	0.47	1.8	1.0	0.63	3.3	0.20	0.91	0.17	0.70	0.19	1.2	0.37	**LOD (ppb)**	3.1	0.80	6.9	17
LOD (fg/m^3)	12	33	6.1	23	13	8.2	4.3	2.6	12	2.2	9.1	2.5	16	4.8	**LOD (pg/m^3)**	40	10	90	220
Sample blank (ppt)	< LOD	< LOD	< LOD	< LOD	< LOD	< LOD	< LOD	< LOD	< LOD	< LOD	< LOD	< LOD	< LOD	< LOD	**Sample blank (ppb)**	260	8.8	< LOD	210
Sample blank (fg/m^3)	< LOD	< LOD	< LOD	< LOD	< LOD	< LOD	< LOD	< LOD	< LOD	< LOD	< LOD	< LOD	< LOD	< LOD	**Sample blank (pg/m^3)**	3400	110	< LOD	2700

LR = Low Resolution; MR = Medium Resolution.

Table 4. Descriptive statistics for PM_{10} samples collected in Ny- Ålesund in 2010 (Bazzano et al., 2016a) and 2011-2013 (this study) and average concentrations of major, minor and trace elements in PM_{10} samples collected in other parts of the world. For calculating mean, median and percentiles, values below the LOD were considered as equal to it; therefore, all mean values except the ones reported for Al, Mg and Na should be intended as < N.

		Al (ng/m^3)	As (pg/m^3)	Ba (pg/m^3)	Ca (ng/m^3)	Cd (pg/m^3)	Co (pg/m^3)	Cu (pg/m^3)	Fe (ng/m^3)	In (pg/m^3)	K (ng/m^3)	Mg (ng/m^3)	Mn (pg/m^3)	Mo (pg/m^3)	Na (ng/m^3)	Ni (pg/m^3)	Pb (pg/m^3)	Ti (pg/m^3)	V (pg/m^3)	Zn (pg/m^3)
NY-ÅLESUND 2010-13	**Mean**	6.56	17	92	20	6.4	6.9	55	6.6	1.5	10	26.7	150	18	170	95	75	300	40	600
	Median	4.96	6.76	54.8	17.0	1.82	2.01	43.4	5.03	1.05	7.65	20.8	109	7.59	137	63.6	29.5	183	18.0	276
	Min	0.290	< 0.029	< 2.2	< 0.56	< 0.0035	< 0.015	< 0.32	< 0.34	< 0.00011	< 0.0017	0.961	< 3.7	< 0.36	2.93	< 0.029	< 0.030	< 1.9	< 0.21	< 2.1
	Max	62.2	242	1020	75.3	125	16.0	608	56.2	24.8	148	143	1320	125	1010	406	1220	4340	585	18000
	5th percentile	0.541	1.4	13	5.1	0.35	0.053	1.2	0.78	0.048	0.63	7.77	17	2.0	33.6	6.5	0.032	25	0.78	47
	95th percentile	16.8	59.1	193	39.0	28.6	11.9	122	14.3	3.38	26.7	60.2	400	78.7	353	311	381	774	180	1320
COMPARISON	**Abramov Glacier (Kyrgyzstan)** [1]	709	5400	$6\cdot10^6$	-	-	300	11800	1650	-	-	-	30000	-	80.10	10000	-	-	14000	13000
	Antalya (Turkey) [2]	354	600	6860	775	170	130	-	193	3000	245	363	6000	-	1296	1750	38000	17000	2140	9400
	New Zealand's Southern Alps [3]	-	5.6	1510	-	17.8	30.7	192	-	0.1	-	-	-	14.6	-	371	163	4917	119	-
	Terra Nova Bay (Antarctica)	7.75 [4]	-	60.9 [4]	-	4.30 [5]	5.09 [4]	410 [5]	6.58 [4]	-	-	-	147 [4]	-	-	-	33.0 [5]	-	22 [4]	109 [4]
	Turin (Italy) [6]	137	380	16700	482	310	180	3900	356	-	232	148	8230	1090	-	6450	6060	18500	1440	37900

		9. La (fg/m^3)	10. Ce (fg/m^3)	Pr (fg/m^3)	Nd (fg/m^3)	Sm (fg/m^3)	Eu (fg/m^3)	Gd (fg/m^3)	Tb (fg/m^3)	Dy (fg/m^3)	Ho (fg/m^3)	Er (fg/m^3)	Yb (fg/m^3)
NY-ÅLESUND 2010-13	**Mean**	2400	5300	510	1800	400	150	440	82	260	39	160	130
	Median	1150	2330	264	820	209	68.7	199	32.9	139	18.9	80.7	67.7
	Min	< 10	< 60	< 3.6	< 15	< 4.1	< 4.7	< 5.9	< 1.4	< 5.9	< 1.0	< 3.0	< 3.4
	Max	28500	52900	4430	17200	3510	958	4030	640	1910	484	1030	880
	5th percentile	52	100	26	33	14	12	15	1.8	13	1.5	10	9.3
	95th percentile	8550	19000	2100	8280	1560	648	1940	304	969	123	627	507
	Antalya (Turkey) [2]	240000	450000	56000	210000	44000	-	47000	6000	35000	7000	20000	18000
	Mexico City (Mexico) [7]	1167000	1402000	205000	596000	81000	22000	79000	6000	42000	9000	30000	40000
	New Zealand's Southern Alps [2]	31700	67900	7900	29800	6000	1200	5200	800	4600	900	2600	2400
	Turin (Italy) [6]	20000	150000	-	-	-	-	-	-	-	-	-	-

[1] Mean values for PM_{10} samples collected in remote areas in 1996/1997 (Kulmatov and Hojamberdiev, 2010).
[2] Median values for PM_{10} samples collected in a remote area in 1993/2001 (Öztürk et al., 2012).
[3] Mean values for TSP samples collected in a remote area in 2009 (Marx et al., 2014).
[4] Median values for PM_{10} samples collected in a remote area in 2001/2002 (Toscano et al., 2005).
[5] Median values for PM_{10} samples collected in a remote area in 2000/2001 (Truzzi et al., 2017).
[6] Mean values for PM_{10} samples collected in a rural area ("DR") in 2011 (Padoan et al., 2016).
[7] Median values for PM_{10} samples collected in a rural area ("T2") in 2006 (Moreno et al., 2008b).

Figure 1. Satellite view of Svalbard Islands and Ny-Ålesund, showing the position of Gruvebadet sampling station.

Figure 2. Ce-La-V ternary diagram for 2010-2013 samples.

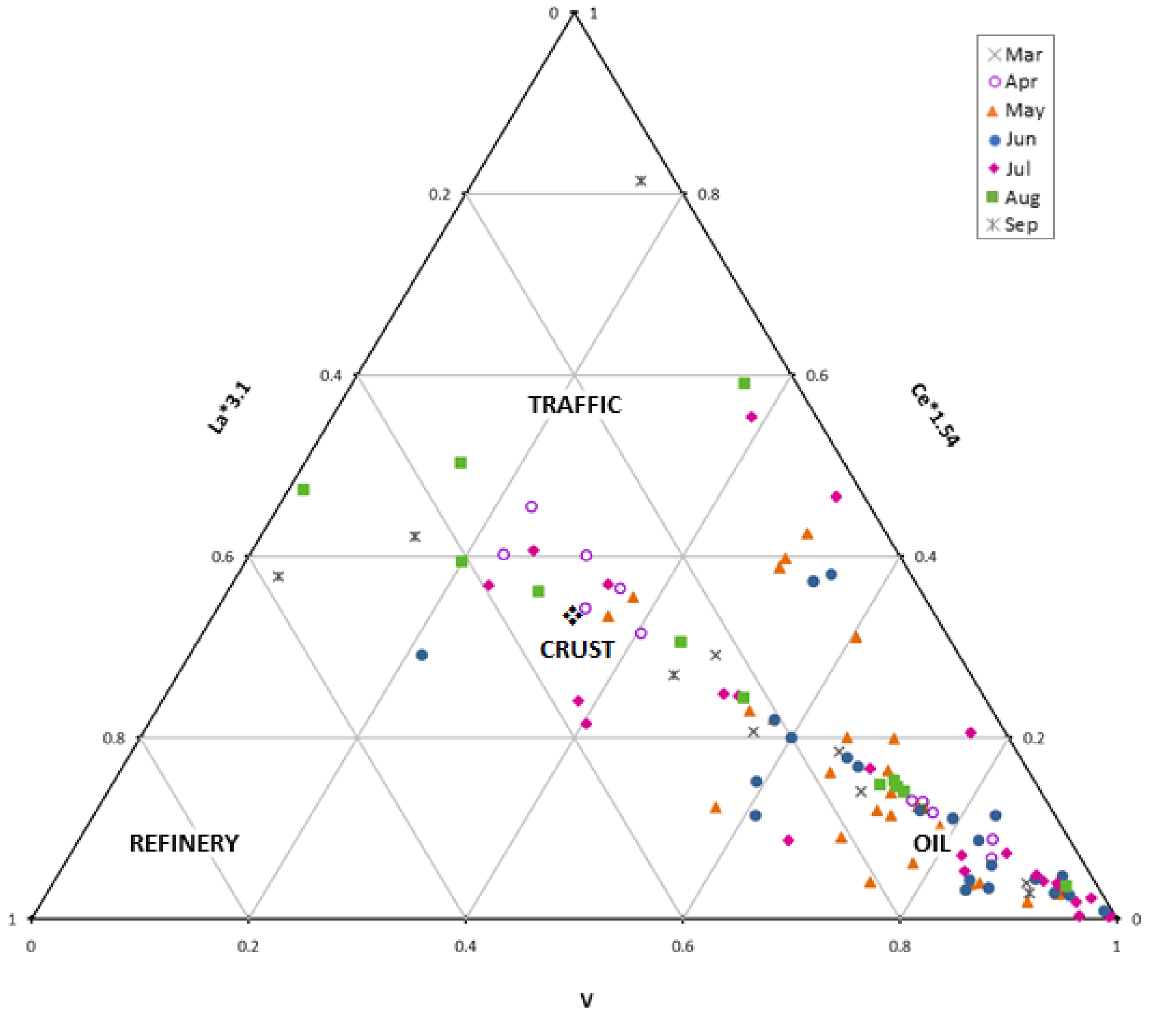

Figure 3. Box plots of a-b) crustal enrichment factors calculated on all samples with respect to the mean crust composition reported by Wedepohl, 1995; c-d) marine enrichment factors calculated on all samples with respect to the sea water composition reported by Goldberg (1965) and Miyazaki (2008).

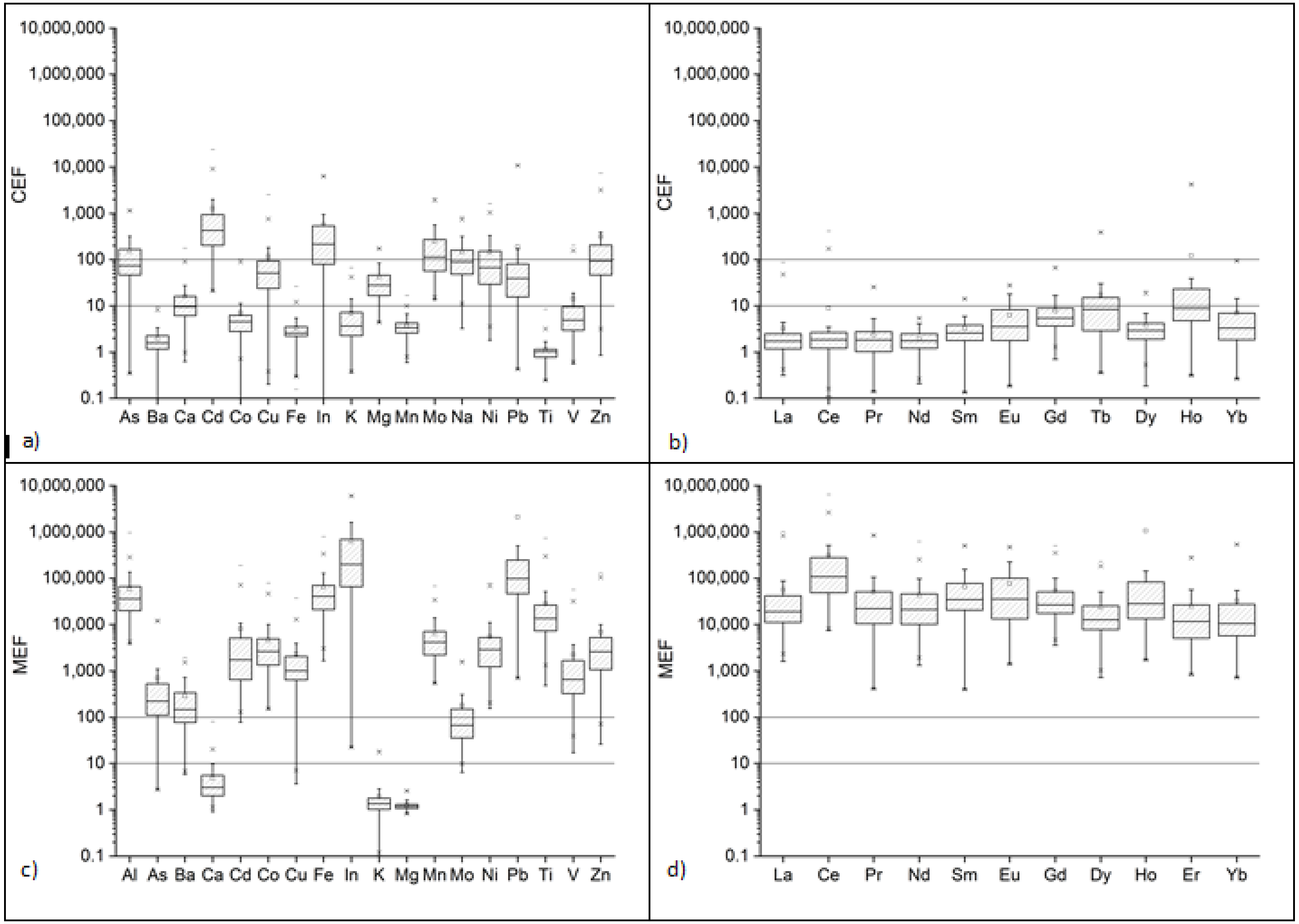

Figure 4. Principal Component Analysis (PC1 vs. PC2) for 2012 samples: a) score plot; b) loading plot.

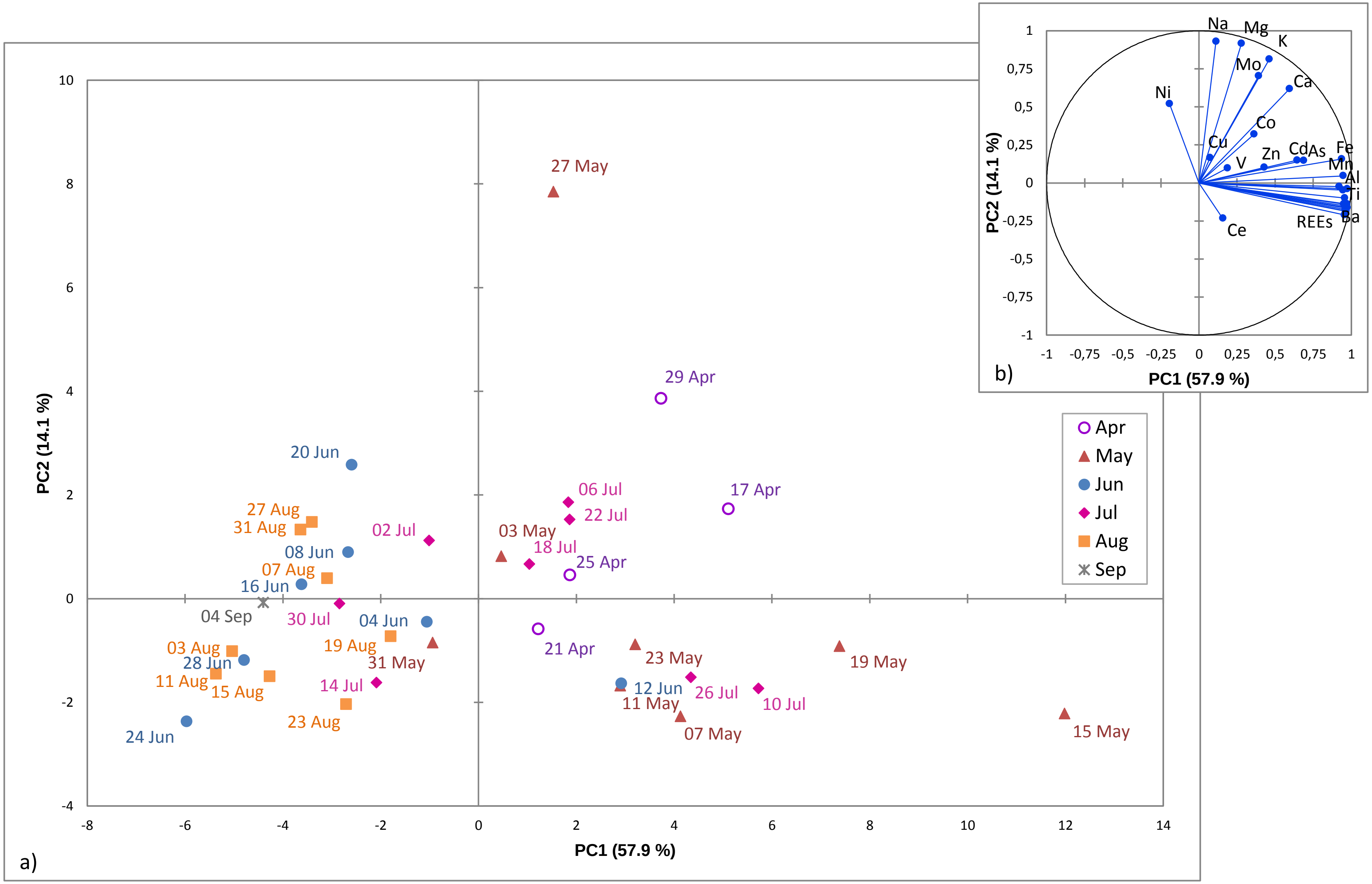

Figure 5. HYSPLIT back-trajectories calculated for two samples collected in 2012: a) 15 May; b) 3 Aug.

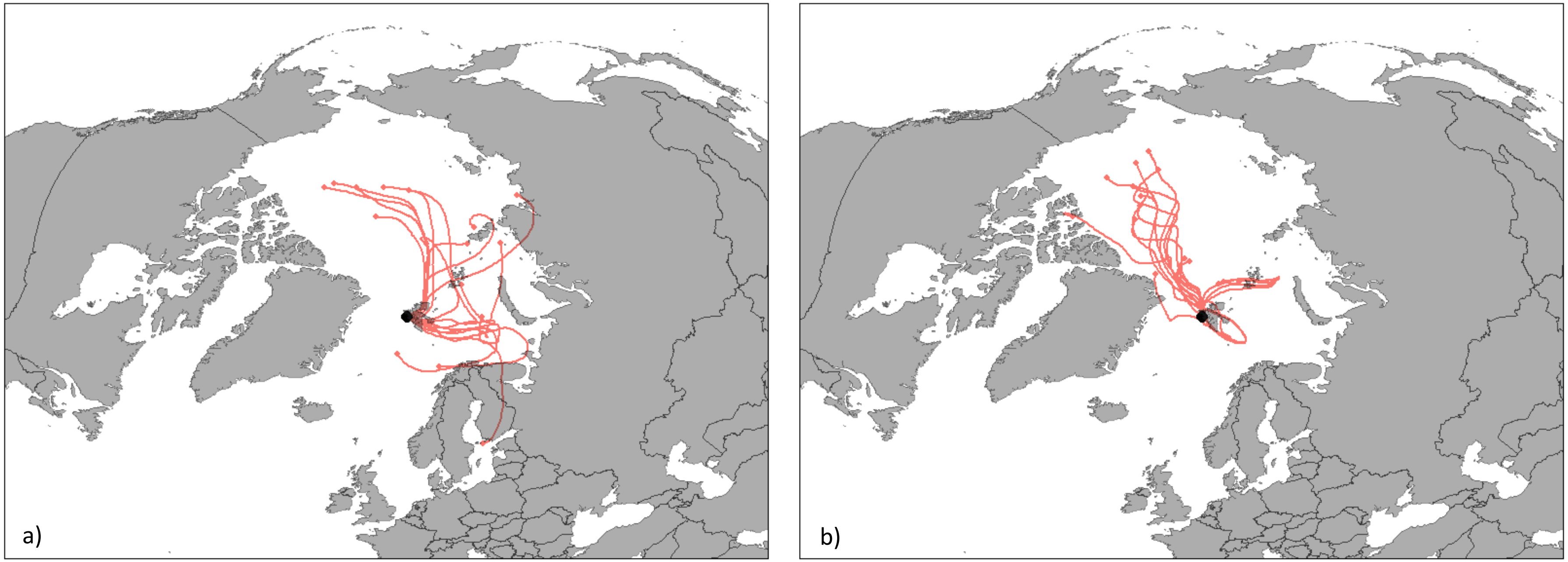

Figure 6. Dendrogram obtained by Q-mode Hierarchical Cluster Analysis for 2012 samples.

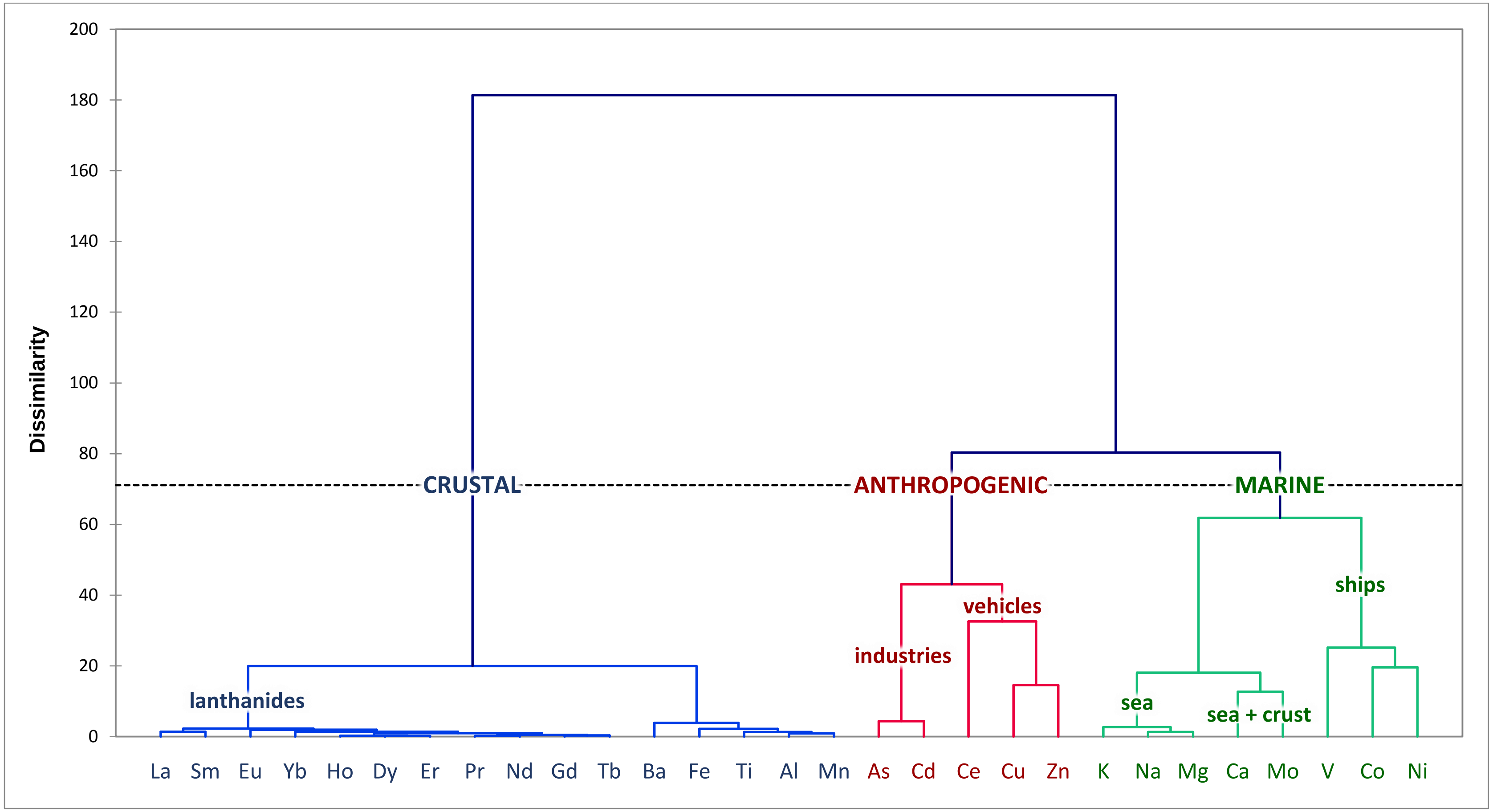

Figure 7. Seasonal trends of As, Cd, Pb and Zn in 2012.

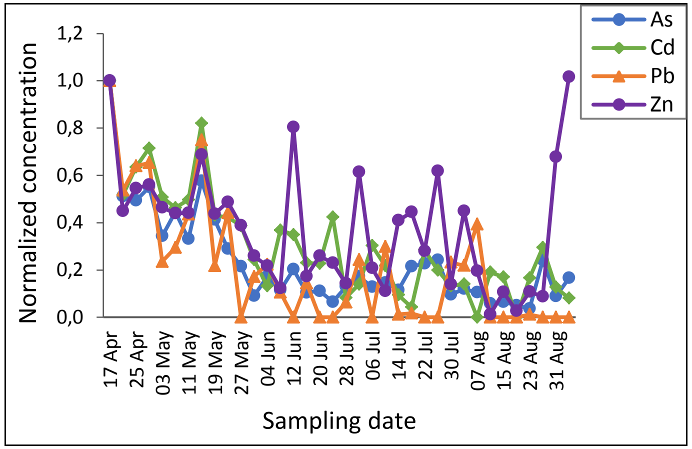

Figure 8. Comprehensive Principal Component Analysis (PC2 vs. PC3) for 2010-2013 samples: a) score plot; b) loading plot.

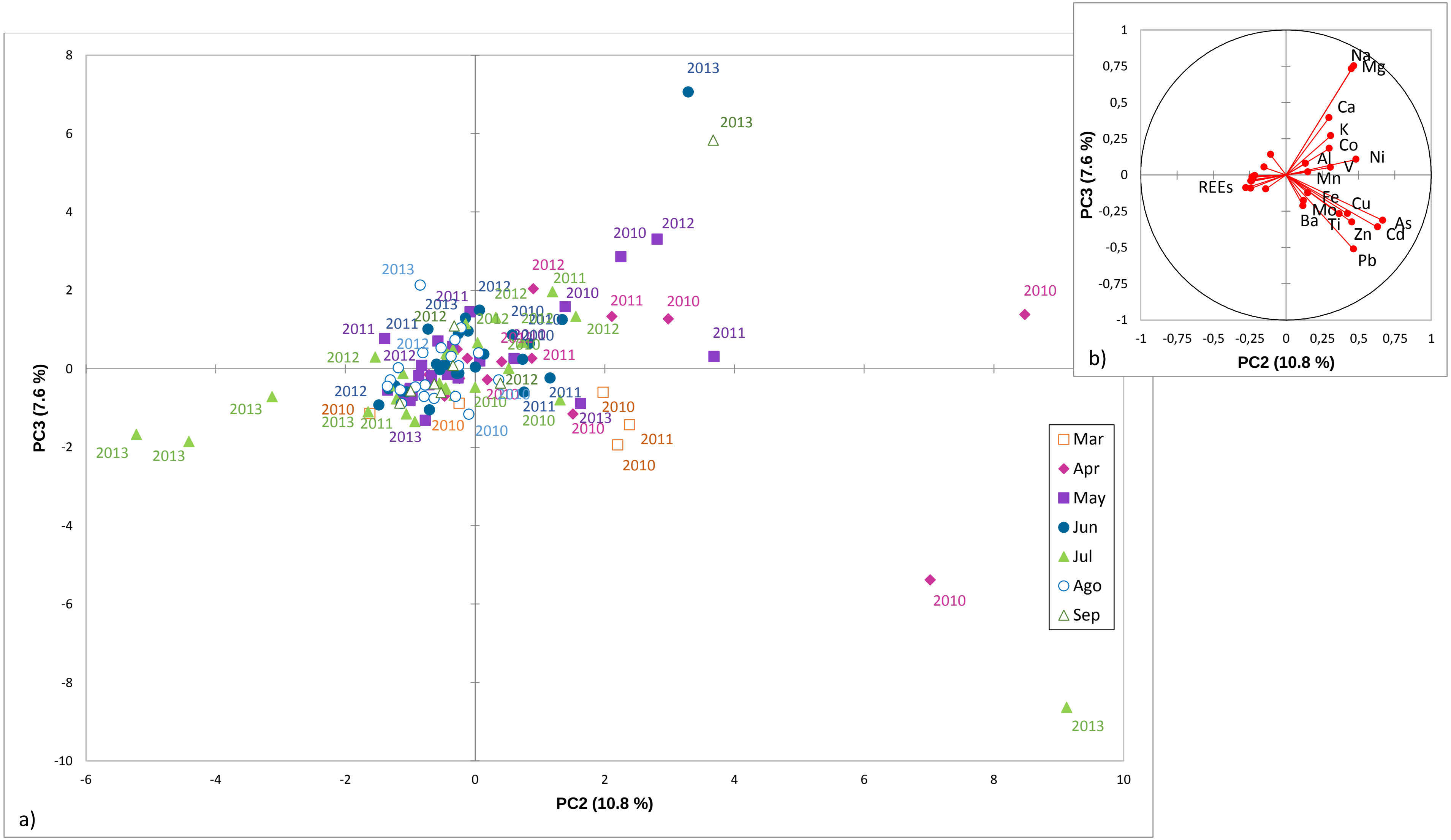

Figure 9. REE patterns: a) mean lanthanides concentration; b) mean shale-normalized concentration; c) mean shale-normalized concentration for each month of 2012 sampling campaign; d) Pr/Yb ratio; e) Ce anomaly; f) Eu anomaly.

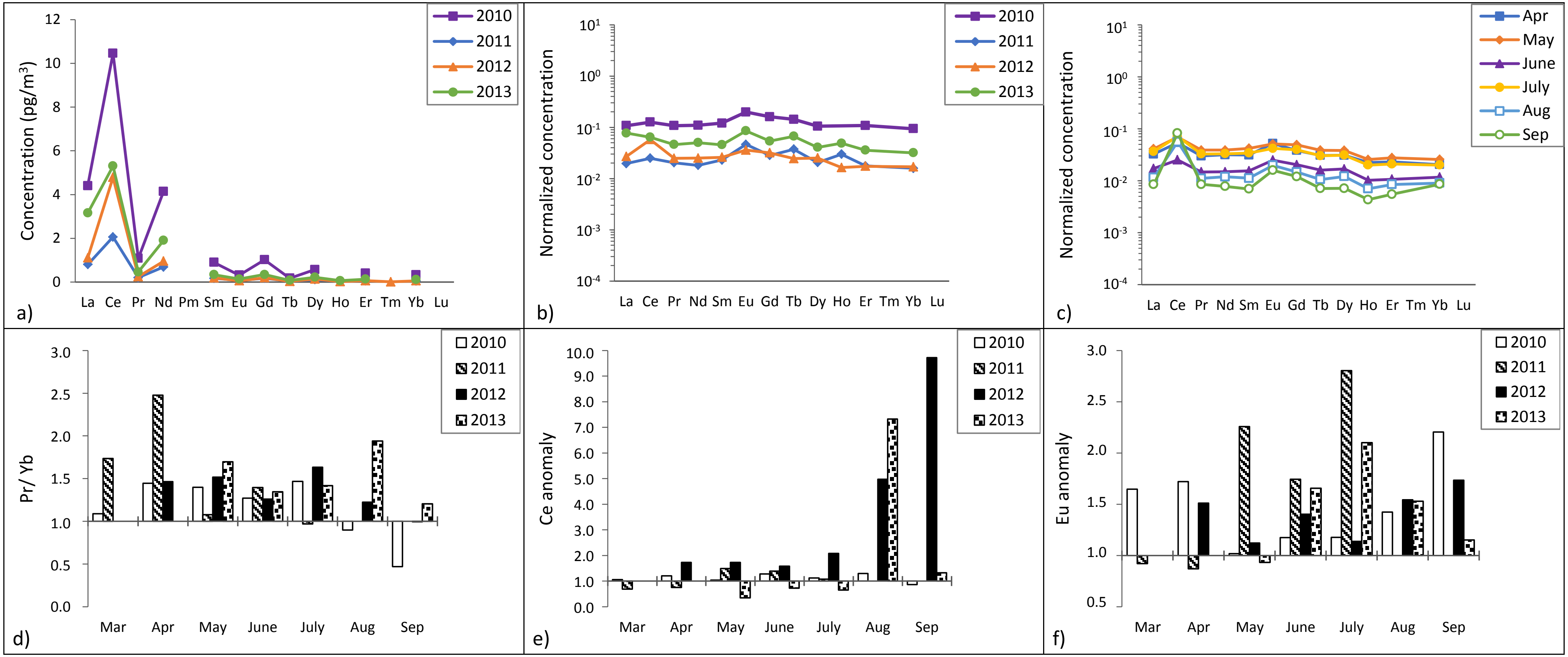

Highlights

- Natural (geogenic and marine) and anthropogenic PM_{10} sources were identified.
- Anthropic element concentrations show a seasonal trend with maxima in spring.
- Airborne pollution from ship emissions was occasionally registered in summer.
- Anthropogenic element concentrations did not change over the examined years.

SUPPLEMENTARY MATERIAL

Supplementary Table 1. Major and minor analyte concentrations determined in PM_{10} samples collected in a) 2011; b) 2012; c) 2013.

a) **2011 CAMPAIGN**

Start date	Al (ng/m^3)	As (pg/m^3)	Ba (pg/m^3)	Ca (ng/m^3)	Cd (pg/m^3)	Co (pg/m^3)	Cu (pg/m^3)	Fe (ng/m^3)	K (ng/m^3)	Mg (ng/m^3)	Mn (pg/m^3)	Mo (pg/m^3)	Na (ng/m^3)	Ni (pg/m^3)	Pb (pg/m^3)	Ti (pg/m^3)	V (pg/m^3)	Zn (pg/m^3)
29 Mar	5.00 ± 0.04	149 ± 6	53 ± 2	18.4 ± 0.2	19.8 ± 0.2	8.21 ± 0.05	130 ± 3	7.6 ± 0.3	5.1 ± 0.9	16.3 ± 0.1	284 ± 7	4.1 ± 0.4	74 ± 1	193 ± 5	470 ± 10	114 ± 5	40.9 ± 0.8	1140 ± 20
03 Apr	10.1 ± 0.1	50 ± 4	44 ± 2	32.63 ± 0.08	8.8 ± 0.1	10.2 ± 0.2	76 ± 3	11.3 ± 0.2	14 ± 2	51.4 ± 0.3	357 ± 8	11.9 ± 0.8	251 ± 3	350 ± 10	181 ± 6	213 ± 6	61 ± 2	1330 ± 30
07 Apr	7.65 ± 0.04	40.8 ± 0.8	53 ± 2	29.8 ± 0.2	7.9 ± 0.2	6.84 ± 0.06	65 ± 2	10.5 ± 0.2	7.9 ± 0.5	31.5 ± 0.2	336 ± 4	4.5 ± 0.4	138 ± 2	195 ± 7	190 ± 6	242 ± 9	56 ± 1	1080 ± 20
11 Apr	1.82 ± 0.02	5.8 ± 0.2	27.4 ± 0.8	14.1 ± 0.3	< 0.20	< 0.045	30.4 ± 0.2	2.36 ± 0.04	5 ± 1	n.a.	63.7 ± 0.8	3.2 ± 0.3	139 ± 2	105 ± 3	47.4 ± 0.5	49 ± 1	7.4 ± 0.2	61 ± 2
01 May	5.46 ± 0.05	< 6.9	< SB	14.7 ± 0.2	3.7 ± 0.2	7.9 ± 0.2	53 ± 2	5.0 ± 0.1	8.7 ± 0.5	36.2 ± 0.4	140 ± 2	3.6 ± 0.2	227 ± 5	153 ± 9	54 ± 2	98 ± 4	24.0 ± 0.8	< SB
05 May	11.3 ± 0.2	29 ± 2	74 ± 3	39.17 ± 0.09	5.5 ± 0.2	7.6 ± 0.1	64.1 ± 0.9	11.6 ± 0.2	13.9 ±0.4	46.5 ± 0.8	243 ± 8	3.1 ± 0.2	263 ± 2	< SB	120 ± 4	329 ± 5	30.6 ± 0.8	399 ± 9
09 May	6.09 ± 0.01	24 ± 2	133 ± 2	60.9 ± 0.7	31 ± 1	4.4 ± 0.1	608 ± 8	6.80 ± 0.05	148 ± 7	28.86 ± 0.09	341 ± 6	17.7 ± 0.8	236 ± 2	400 ± 30	161 ± 4	153 ± 4	16.8 ± 0.7	4140 ± 80
13 May	7.37 ± 0.06	16.1 ± 0.4	76 ± 2	35.7 ± 0.2	3.9 ± 0.1	5.7 ± 0.1	91 ± 3	10.2 ± 0.2	11 ± 1	47.3 ± 0.1	238 ± 6	3.0 ± 0.2	298 ± 3	< SB	67 ± 3	168 ± 6	21.9 ± 0.7	890 ± 20
17 May	12.0 ± 0.1	18 ± 1	64 ± 2	22.3 ± 0.1	7.0 ± 0.3	5.7 ± 0.1	59 ± 2	10.9 ± 0.3	7 ± 1	22.6 ± 0.2	191 ± 4	30.1 ± 0.9	117.2 ± 0.8	< SB	66 ± 2	233 ± 7	22.2 ± 0.4	440 ± 10
21 May	7.9 ± 0.1	11.3 ± 0.7	2.16 ± 0.03	23.8 ± 0.3	< 4.5	6.7 ± 0.2	112 ± 2	5.7 ± 0.4	12.8 ± 0.3	22.8 ± 0.1	155 ± 6	6.1 ± 0.3	111 ± 2	6.8 ± 0.4	33.9 ± 0.7	160 ± 3	18 ± 1	< SB
25 May	3.59 ± 0.02	< 6.0	10.4 ± 0.3	11.3 ± 0.2	1.58 ± 0.03	4.49 ± 0.09	57 ± 2	4.8 ± 0.3	3.0 ± 0.6	16.63 ± 0.02	85 ± 3	0.88 ± 0.07	85 ± 2	63 ± 2	23 ± 1	66 ± 3	10.8 ± 0.7	2.08 ± 0.06
29 May	2.82 ± 0.01	< 5.2	46 ± 2	14.0 ± 0.2	1.74 ± 0.06	4.95 ± 0.09	78 ± 1	4.05 ± 0.09	< 0.056	9.73 ± 0.08	78 ± 1	2.0 ± 0.2	34.3 ± 0.8	< SB	17.1 ± 0.5	71 ± 1	12.9 ± 0.2	175 ± 5
05 Jun	2.62 ± 0.02	58 ± 4	17.2 ± 0.5	22.3 ± 0.3	27.3 ± 0.5	3.7 ± 0.1	53 ± 2	2.54 ± 0.03	6.6 ± 0.3	28.3 ± 0.2	59 ± 1	91 ± 3	185 ± 4	< 6.2	1.41 ± 0.05	96 ± 3	7.0 ± 0.5	247 ± 5
09 Jun	1.92 ± 0.02	< 5.8	< SB	22.7 ± 0.4	1.8 ± 0.1	2.7 ± 0.1	30 ± 2	1.98 ± 0.01	8.0 ± 0.5	36.1 ± 0.3	48 ± 1	< 0.64	258 ± 2	< 6.4	< 5.5	34 ± 2	5.4 ± 0.2	252 ± 6
13 Jun	10.7 ± 0.1	16 ± 1	41.4 ± 0.8	53.2 ± 0.5	15.1 ± 0.6	9.4 ± 0.3	51.0 ± 0.5	14.3 ± 0.1	26.7 ± 0.4	36.52 ± 0.09	328 ± 3	10.8 ± 0.7	202.1 ± 0.8	78 ± 4	61 ± 1	380 ± 10	134 ± 5	1200 ± 30
17 Jun	6.40 ± 0.08	138 ± 5	10.0 ± 0.1	28.7 ± 0.7	6.8 ± 0.2	5.1 ± 0.2	34.7 ± 0.6	5.96 ± 0.04	23.8 ± 0.7	21.16 ± 0.07	130 ± 1	6.6 ± 0.6	118 ± 2	90 ± 4	30.1 ± 0.5	182 ± 5	125 ± 3	103 ± 2
21 Jun	2.03 ± 0.02	23 ± 1	< SB	16.0 ± 0.2	< 0.60	1.82 ± 0.08	< 2.5	4.06 ± 0.06	14.3 ± 0.6	4.29 ± 0.07	21.4 ± 0.4	2.9 ± 0.3	21.0 ± 0.4	< SB	< 5.5	36.9 ± 0.8	3.5 ± 0.5	< SB
25 Jun	2.383 ± 0.008	< 7.6	< SB	20.0 ± 0.4	< 0.79	1.88 ± 0.07	56.7 ± 0.8	2.04 ± 0.02	1.9 ± 0.4	10.5 ± 0.2	39 ± 1	8.1 ± 0.6	45.6 ± 0.3	< SB	< SB	40 ± 2	13.3 ± 0.4	< SB
29 Jun	2.85 ± 0.04	< 5.9	< SB	9.5 ± 0.2	< 0.61	2.35 ± 0.03	82 ± 2	2.33 ± 0.02	< SB	12.8 ± 0.1	46 ± 1	3.5 ± 0.2	63.5 ± 0.9	6.3 ± 0.3	< SB	46 ± 3	6.7 ± 0.3	< 55
03 Jul	2.38 ± 0.02	< 5.9	< SB	24.7 ± 0.4	< 0.60	6.2 ± 0.2	125 ± 2	3.50 ± 0.02	15.2 ± 0.3	50.3 ± 0.5	54.4 ± 0.9	6.5 ± 0.4	361 ± 4	108 ± 5	1.19 ± 0.02	69 ± 2	181 ± 2	< SB
07 Jul	2.33 ± 0.01	< 5.8	< SB	38.7 ± 0.2	< 0.60	1.59 ± 0.07	40 ± 1	1.95 ± 0.02	8 ± 3	20.1 ± 0.1	46 ± 1	3.8 ± 0.2	121 ± 2	44 ± 3	32.2 ± 0.7	55 ± 3	247 ± 9	330 ± 10
15 Jul	0.910 ± 0.008	< 5.9	< SB	4.8 ± 0.1	28.5 ± 0.9	0.38 ± 0.02	8.71 ± 0.07	0.82 ± 0.01	< 0.063	3.69 ± 0.06	3.7 ± 0.1	2.6 ± 0.1	14.5 ± 0.4	< 6.5	< SB	< SB	2.3 ± 0.1	< SB
19 Jul	1.51 ± 0.01	< 5.9	< SB	18.5 ± 0.2	< 0.61	1.21 ± 0.06	38.8 ± 0.8	0.890 ± 0.007	10.5 ± 0.6	8.40 ± 0.06	16.9 ± 0.4	2.5 ± 0.2	40.87 ± 0.08	< SB	< SB	1.90 ± 0.08	3.0 ± 0.1	97 ± 3
23 Jul	4.10 ± 0.03	< 5.9	3.15 ± 0.05	30.3 ± 0.7	< 0.61	3.5 ± 0.1	35.6 ± 0.3	3.10 ± 0.08	27 ± 5	32.0 ± 0.2	61 ± 2	5.3 ± 0.2	191 ± 1	7.5 ± 0.2	< SB	105 ± 5	48 ± 3	< 56

SB = Sample Blank; n.a. = not analysed. Values below the LOD were obtained by using the real solution volume and air volume of each sample.

b)										2012 CAMPAIGN									
Start date	**Al (ng/m^3)**	**As (pg/m^3)**	**Ba (pg/m^3)**	**Ca (ng/m^3)**	**Cd (pg/m^3)**	**Co (pg/m^3)**	**Cu (pg/m^3)**	**Fe (ng/m^3)**	**In (fg/m^3)**	**K (ng/m^3)**	**Mg (ng/m^3)**	**Mn (pg/m^3)**	**Mo (pg/m^3)**	**Na (ng/m^3)**	**Ni (pg/m^3)**	**Pb (pg/m^3)**	**Ti (pg/m^3)**	**V (pg/m^3)**	**Zn (pg/m^3)**
17 Apr	9.6 ± 0.3	48 ± 3	104 ± 4	21.1 ± 0.2	5.1 ± 0.8	3.2 ± 0.2	106 ± 2	8.7 ± 0.2	< 27	12.6 ± 0.1	38 ± 1	231 ± 5	11.4 ± 0.6	210 ± 20	77 ± 3	168 ± 6	370 ± 10	34 ± 2	560 ± 20
21 Apr	5.8 ± 0.2	25 ± 1	77 ± 2	16.4 ± 0.5	2.7 ± 0.4	1.19 ± 0.01	31.0 ± 0.9	5.6 ± 0.1	< 24	8.1 ± 0.1	22.5 ± 0.7	154 ± 4	5.4 ± 0.4	140 ± 20	28 ± 2	90 ± 1	224 ± 6	21 ± 2	251 ± 6
25 Apr	6.4 ± 0.2	24 ± 2	78 ± 3	17.3 ± 0.1	3.3 ± 0.7	1.23 ± 0.02	43 ± 2	6.32 ± 0.08	< 24	11.79 ± 0.03	35.2 ± 0.3	159 ± 5	5.8 ± 0.4	220 ± 10	40 ± 3	107 ± 2	278 ± 8	26.2 ± 0.8	300 ± 20
29 Apr	7.4 ± 0.4	26 ± 3	105 ± 4	29.2 ± 0.2	3.7 ± 0.4	2.36 ± 0.08	82 ± 2	6.74 ± 0.07	< 24	20.8 ± 0.2	68.1 ± 0.9	191 ± 8	6.9 ± 0.4	398 ± 5	52 ± 2	109 ± 3	280 ± 10	28 ± 1	310 ± 10
03 May	4.5 ± 0.4	16 ± 2	64 ± 2	15.9 ± 0.2	2.6 ± 0.4	3.44 ± 0.07	51.3 ± 0.8	4.72 ± 0.08	420 ± 60	12.6 ± 0.4	34 ± 1	121 ± 4	6.2 ± 0.6	230 ± 10	12.7 ± 0.4	40 ± 1	211 ± 6	20 ± 3	260 ± 10
07 May	8.3 ± 0.2	21 ± 1	89 ± 3	12.3 ± 0.1	2.4 ± 0.3	3.4 ± 0.2	24 ± 1	7.86 ± 0.09	350 ± 40	7.17 ± 0.07	15.0 ± 0.2	213 ± 7	6.4 ± 0.5	75 ± 2	9.2 ± 0.5	49 ± 1	370 ± 20	24 ± 1	250 ± 10
11 May	7.4 ± 0.1	15.9 ± 0.8	91 ± 2	14.0 ± 0.3	2.6 ± 0.5	3.8 ± 0.2	65 ± 3	6.8 ± 0.2	460 ± 50	7.05 ± 0.04	16.6 ± 0.4	194 ± 6	4.8 ± 0.3	89 ± 4	12.0 ± 0.8	73 ± 1	317 ± 6	27.6 ± 0.4	247 ± 5
15 May	14.8 ± 0.2	28 ± 2	146 ± 4	16.76 ± 0.06	4.2 ± 0.4	7.1 ± 0.2	45 ± 1	12.4 ± 0.3	420 ± 30	11.9 ± 0.2	20.4 ± 0.3	410 ± 20	7.6 ± 0.6	112 ± 3	21.3 ± 0.8	126 ± 4	680 ± 20	47 ± 3	380 ± 20
19 May	11.8 ± 0.5	20 ± 1	136 ± 5	22.3 ± 0.3	2.2 ± 0.4	4.8 ± 0.3	52 ± 1	9.7 ± 0.4	340 ± 60	11.6 ± 0.3	28.3 ± 0.5	270 ± 10	6.0 ± 0.5	170 ± 10	5.2 ± 0.4	36 ± 2	510 ± 10	32 ± 2	240 ± 10
23 May	7.49 ± 0.05	14 ± 1	103 ± 2	20.82 ± 0.08	2.2 ± 0.5	1.7 ± 0.1	54 ± 1	7.1 ± 0.3	20 ± 3	9.99 ± 0.09	20 ± 1	219 ± 6	4.1 ± 0.5	132 ± 4	60 ± 1	74 ± 1	330 ± 10	14.2 ± 0.1	270 ± 10
27 May	5.6 ± 0.2	10 ± 2	59 ± 1	30.4 ± 0.5	2.0 ± 0.3	12.2 ± 0.3	97 ± 2	9.9 ± 0.3	360 ± 40	21.4 ± 0.2	74 ± 3	207 ± 7	20.9 ± 0.9	510 ± 20	410 ± 20	< 0.030	260 ± 10	22.6 ± 0.5	220 ± 10
31 May	5.7 ± 0.2	4.4 ± 0.5	48 ± 1	14.62 ± 0.09	1.3 ± 0.4	6.2 ± 0.2	54 ± 1	6.8 ± 0.1	< 27	6.05 ± 0.08	18.2 ± 0.5	148 ± 2	2.9 ± 0.4	110 ± 3	92 ± 2	28.9 ± 0.7	258 ± 3	15.2 ± 0.2	145 ± 9
04 Jun	5.0 ± 0.1	8.2 ± 0.4	68 ± 2	16.0 ± 0.2	0.7 ± 0.2	1.60 ± 0.08	45 ± 2	4.73 ± 0.06	< 26	7.7 ± 0.2	22.7 ± 0.9	125 ± 4	3.2 ± 0.3	158 ± 3	87 ± 3	37.4 ± 0.7	238 ± 6	11.3 ± 0.3	121 ± 6
08 Jun	2.8 ± 0.1	5.5 ± 0.4	37 ± 1	16.3 ± 0.2	1.9 ± 0.5	3.7 ± 0.2	7.4 ± 0.2	2.71 ± 0.09	200 ± 20	10.4 ± 0.1	31 ± 1	64 ± 2	2.8 ± 0.2	250 ± 10	84 ± 2	17.7 ± 0.6	127 ± 5	71 ± 2	68 ± 5
12 Jun	6.1 ± 0.3	9.7 ± 0.7	83 ± 2	26.44 ± 0.08	1.8 ± 0.5	2.55 ± 0.06	60 ± 2	5.7 ± 0.2	410 ± 20	4.5 ± 0.2	12.3 ± 0.3	139 ± 6	7.3 ± 0.9	47 ± 1	31 ± 2	< 0.033	210 ± 10	87 ± 4	450 ± 30
16 Jun	2.37 ± 0.08	5.0 ± 0.5	36.4 ± 0.8	11.6 ± 0.1	1.2 ± 0.3	0.26 ± 0.02	49 ± 1	2.40 ± 0.05	< 27	7.34 ± 0.09	22.7 ± 0.6	65.8 ± 0.8	2.1 ± 0.2	173 ± 3	350 ± 10	24.3 ± 0.5	95 ± 4	13.3 ± 0.2	97 ± 5
20 Jun	1.76 ± 0.05	5.3 ± 0.7	37 ± 1	25.8 ± 0.3	1.2 ± 0.1	1.29 ± 0.04	56 ± 3	2.58 ± 0.06	470 ± 40	12.41 ± 0.09	42.5 ± 0.9	57 ± 2	7.6 ± 0.8	341 ± 7	49 ± 2	< 0.033	92 ± 5	13.4 ± 0.8	145 ± 5
24 Jun	0.290 ± 0.007	3.1 ± 0.8	12.8 ± 0.3	8.83 ± 0.06	2.2 ± 0.9	< 0.016	5.2 ± 0.2	0.34 ± 0.01	160 ± 7	0.39 ± 0.02	0.96 ± 0.02	3.95 ± 0.08	0.36 ± 0.07	2.93 ± 0.05	37.8 ± 0.8	< 0.034	2.9 ± 0.2	< 0.21	128 ± 5
28 Jun	0.94 ± 0.01	6 ± 1	23.2 ± 0.5	5.727 ± 0.009	0.4 ± 0.1	12.5 ± 0.5	5.8 ± 0.1	1.66 ± 0.04	< 27	2.49 ± 0.06	7.9 ± 0.1	25 ± 1	2.2 ± 0.2	58.8 ± 0.7	116 ± 2	10.6 ± 0.6	37 ± 1	128 ± 3	80 ± 3
02 Jul	4.55 ± 0.09	8.3 ± 0.6	46 ± 1	17.64 ± 0.04	0.7 ± 0.1	3.8 ± 0.1	68 ± 2	5.31 ± 0.08	< 28	10.2 ± 0.2	31.9 ± 0.7	110 ± 4	5.8 ± 0.4	237 ± 3	99 ± 3	41 ± 1	300 ± 100	34.6 ± 0.5	340 ± 10
06 Jul	5.3 ± 0.2	6.2 ± 0.8	54 ± 2	20.8 ± 0.1	1.6 ± 0.4	4.6 ± 0.2	56 ± 2	5.88 ± 0.05	330 ± 50	12.5 ± 0.2	39.0 ± 0.7	123 ± 1	11.4 ± 0.7	300 ± 10	200 ± 10	< 0.032	180 ± 10	128 ± 9	116 ± 9
10 Jul	7.7 ± 0.2	7 ± 1	80 ± 2	22.6 ± 0.5	1.1 ± 0.2	2.9 ± 0.1	42.9 ± 0.9	7.7 ± 0.2	300 ± 100	9.2 ± 0.3	28.8 ± 0.5	163 ± 4	4.1 ± 0.4	180 ± 6	9.4 ± 0.5	50 ± 2	260 ± 10	32 ± 1	62 ± 3
14 Jul	3.1 ± 0.2	6 ± 1	43.9 ± 0.8	13.72 ± 0.09	0.5 ± 0.1	0.95 ± 0.07	18.4 ± 0.4	2.95 ± 0.09	< 27	5.312 ± 0.009	14 ± 2	64 ± 2	3.2 ± 0.5	91 ± 4	64 ± 2	2.07 ± 0.05	175 ± 7	64 ± 1	230 ± 10
18 Jul	6.8 ± 0.1	10.3 ± 0.9	51 ± 1	17.0 ± 0.2	0.22 ± 0.04	10.5 ± 0.4	44 ± 1	7.3 ± 0.2	< 28	8.25 ± 0.07	24.4 ± 0.5	141 ± 2	4.9 ± 0.4	161 ± 4	396 ± 7	2.87 ± 0.06	327 ± 5	80.3 ± 0.5	250 ± 10
22 Jul	5.5 ± 0.1	10.9 ± 0.9	64 ± 2	19.9 ± 0.4	1.5 ± 0.2	6.8 ± 0.3	70 ± 2	5.4 ± 0.2	350 ± 30	10.4 ± 0.1	33.6 ± 0.7	110 ± 2	9.8 ± 0.8	250 ± 20	247 ± 9	< 0.032	200 ± 10	580 ± 20	157 ± 9
26 Jul	7.1 ± 0.3	11.6 ± 0.5	84 ± 2	19.6 ± 0.3	1.0 ± 0.4	5.8 ± 0.3	192 ± 3	7.29 ± 0.08	380 ± 30	5.7 ± 0.1	17.0 ± 0.4	144 ± 1	6.7 ± 0.5	80 ± 4	87 ± 3	< 0.032	259 ± 9	177 ± 9	350 ± 20
30 Jul	3.89 ± 0.05	4.6 ± 0.8	35.6 ± 0.8	13.8 ± 0.1	0.7 ± 0.2	2.6 ± 0.1	32.8 ± 0.6	4.19 ± 0.09	< 25	7.01 ± 0.07	22.6 ± 0.3	82 ± 1	5.6 ± 0.5	163 ± 3	134 ± 3	38.9 ± 0.9	169 ± 2	10.2 ± 0.3	78 ± 3
03 Aug	1.40 ± 0.03	5.8 ± 0.4	37.4 ± 0.8	8.84 ± 0.09	0.7 ± 0.1	0.60 ± 0.02	78 ± 2	1.23 ± 0.01	30 ± 2	1.97 ± 0.08	8.5 ± 0.3	23.4 ± 0.5	7.1 ± 0.7	52.3 ± 0.2	110 ± 3	37 ± 1	25 ± 2	18.0 ± 0.3	251 ± 10
07 Aug	2.7 ± 0.1	5.0 ± 0.3	53 ± 1	12.8 ± 0.1	< 0.0035	2.5 ± 0.1	44.7 ± 0.7	3.58 ± 0.09	< 26	6.2 ± 0.3	19.0 ± 0.4	68 ± 2	10.4 ± 0.6	137 ± 4	218 ± 4	66 ± 1	123 ± 2	8.1 ± 0.3	109 ± 5
11 Aug	0.44 ± 0.03	2.8 ± 0.2	21 ± 1	7.81 ± 0.09	1.0 ± 0.3	< 0.017	13.9 ± 0.3	1.41 ± 0.03	300 ± 100	4.08 ± 0.01	13.1 ± 0.3	22.6 ± 0.8	3.7 ± 0.3	105 ± 4	97 ± 2	< 0.036	20 ± 1	< 0.23	7.1 ± 0.5
15 Aug	1.50 ± 0.07	3.1 ± 0.6	16.0 ± 0.6	9.36 ± 0.04	0.9 ± 0.3	0.20 ± 0.01	14.5 ± 0.4	1.93 ± 0.04	290 ± 40	4.4 ± 0.1	15.5 ± 0.4	37 ± 1	2.4 ± 0.2	100 ± 5	< 0.029	< 0.030	85 ± 6	6.7 ± 0.1	59 ± 4
19 Aug	3.51 ± 0.07	2.4 ± 0.7	41 ± 2	14.00 ± 0.06	< 0.0035	0.41 ± 0.02	15.1 ± 0.3	3.81 ± 0.05	< 26	8.09 ± 0.07	24.4 ± 0.9	82.9 ± 0.7	1.2 ± 0.2	191 ± 7	127 ± 4	< 0.031	164 ± 7	7.67 ± 0.07	15.2 ± 0.8
23 Aug	2.65 ± 0.06	1.8 ± 0.3	44 ± 1	9.43 ± 0.08	0.9 ± 0.2	< 0.015	32.3 ± 0.5	2.50 ± 0.03	< 27	4.45 ± 0.09	12.9 ± 0.4	61 ± 2	1.3 ± 0.2	85 ± 2	61 ± 2	1.94 ± 0.05	108 ± 2	3.82 ± 0.07	60 ± 4
27 Aug	1.24 ± 0.03	12 ± 1	24.6 ± 0.7	18.2 ± 0.1	1.5 ± 0.3	0.93 ± 0.03	75 ± 1	2.01 ± 0.05	400 ± 60	11.92 ± 0.06	36.2 ± 0.7	33 ± 2	6.7 ± 0.5	267 ± 9	48 ± 3	< 0.031	34 ± 3	9.2 ± 0.1	49 ± 2
31 Aug	1.17 ± 0.02	4.3 ± 0.3	22.3 ± 0.6	14.7 ± 0.2	0.7 ± 0.2	< 0.014	4.0 ± 0.1	1.48 ± 0.04	< 26	12.7 ± 0.2	34.2 ± 0.7	33.4 ± 0.9	3.1 ± 0.3	321 ± 4	53 ± 4	< 0.031	140 ± 10	7.8 ± 0.3	380 ± 10
04 Sep	0.80 ± 0.02	8 ± 1	21.7 ± 0.5	10.2 ± 0.1	0.4 ± 0.1	< 0.015	372 ± 7	1.09 ± 0.03	< 27	5.9 ± 0.1	20.8 ± 0.4	15.7 ± 0.6	1.7 ± 0.2	151 ± 2	201 ± 6	< 0.031	25 ± 2	3.71 ± 0.07	570 ± 20

Values below the LOD were obtained by using the real solution volume and air volume of each sample.

c) **2013 CAMPAIGN**

Start date	Al (ng/m^3)	As (pg/m^3)	Ba (pg/m^3)	Ca (ng/m^3)	Cd (pg/m^3)	Co (pg/m^3)	Cu (pg/m^3)	Fe (ng/m^3)	In (fg/m^3)	K (ng/m^3)	Mg (ng/m^3)	Mn (pg/m^3)	Mo (pg/m^3)	Na (ng/m^3)	Ni (pg/m^3)	Pb (pg/m^3)	Ti (pg/m^3)	V (pg/m^3)	Zn (pg/m^3)
01 May	11.7 ± 0.2	27 ± 1	170 ± 7	33.9 ± 0.5	2.95 ± 0.2	5.2 ± 0.1	65 ± 1	8.6 ± 0.1	192 ± 5	2.69 ± 0.02	12.9 ± 0.1	209 ± 8	49 ± 2	176 ± 3	10.1 ± 0.2	112 ± 8	500 ± 10	24.0 ± 0.4	430 ± 20
05 May	10.5 ± 0.1	27 ± 1	140 ± 2	17.2 ± 0.3	6.61 ± 0.08	4.5 ± 0.1	117 ± 1	6.35 ± 0.06	178 ± 4	3.88 ± 0.03	36.2 ± 0.1	204 ± 2	34 ± 1	67 ± 1	79 ± 3	206 ± 8	420 ± 10	23.5 ± 0.4	1120 ± 20
09 May	0.97 ± 0.02	1.4 ± 0.2	48.8 ± 0.6	4.57 ± 0.06	< SB	0.88 ± 0.03	91 ± 5	0.63 ± 0.01	< 130	< SB	34.18 ± 0.07	24.6 ± 0.5	4.2 ± 0.2	36.1 ± 0.5	155 ± 5	< 2.8	49.2 ± 0.7	< 0.32	290 ± 10
13 May	9.4 ± 0.1	11.6 ± 0.6	119 ± 2	28.9 ± 0.3	< SB	7.19 ± 0.08	470 ± 20	9.6 ± 0.2	< 150	3.30 ± 0.04	20.8 ± 0.3	144 ± 2	81 ± 1	126 ± 1	360 ± 10	32 ± 2	396 ± 5	7.81 ± 0.08	270 ± 20
17 May	6.9 ± 0.5	16 ± 2	40 ± 2	14.6 ± 0.2	< 0.49	5.7 ± 0.2	< 41	5.9 ± 0.6	1170 ± 10	< SB	29.5 ± 0.3	141 ± 5	22 ± 1	170 ± 1	< 22	19 ± 1	810 ± 40	19.2 ± 0.8	78 ± 1
21 May	5.72 ± 0.09	9.0 ± 0.4	81 ± 2	20.8 ± 0.4	< SB	3.7 ± 0.2	59 ± 3	3.05 ± 0.09	< 140	< SB	13.2 ± 0.2	94 ± 5	34 ± 1	99 ± 1	37 ± 2	17.7 ± 0.9	350 ± 20	17.3 ± 0.7	87 ± 4
25 May	7.3 ± 0.4	4.2 ± 0.2	< 43	11.617 ± 0.009	< SB	2.18 ± 0.05	< 48	1.97 ± 0.04	720 ± 70	< SB	7.8 ± 0.2	40 ± 3	118 ± 4	128 ± 3	21.9 ± 0.5	< 3.5	110 ± 8	3.13 ± 0.05	163 ± 7
29 May	3.35 ± 0.08	6.2 ± 0.3	49 ± 2	21.3 ± 0.5	0.27 ± 0.01	3.3 ± 0.1	75 ± 4	1.51 ± 0.05	< 130	0.453 ± 0.003	21.0 ± 0.2	57.2 ± 0.9	17 ± 1	127.1 ± 0.5	71 ± 3	26.6 ± 0.6	165 ± 9	5.6 ± 0.2	610 ± 20
02 Jun	9.35 ± 0.06	13 ± 1	107 ± 2	28.9 ± 0.4	1.50 ± 0.09	10.4 ± 0.2	80 ± 10	11.06 ± 0.02	< 140	13.8 ± 0.1	25.0 ± 0.5	189 ± 3	22.1 ± 0.8	290 ± 1	154 ± 6	42 ± 2	477 ± 8	19.7 ± 0.1	520 ± 40
06 Jun	25.0 ± 0.9	12.3 ± 0.7	168 ± 3	75.3 ± 0.5	< SB	9.1 ± 0.4	47 ± 2	1.59 ± 0.05	1070 ± 10	30.3 ± 0.4	17 ± 3	300 ± 10	13.8 ± 0.5	1012 ± 7	55.1 ± 0.7	44 ± 1	1110 ± 70	58 ± 2	132 ± 7
10 Jun	5.5 ± 0.3	5.4 ± 0.5	56 ± 2	27.3 ± 0.2	< SB	2.77 ± 0.09	< 39	1.15 ± 0.07	< 130	5.78 ± 0.02	16.5 ± 0.2	71 ± 2	13.8 ± 0.9	306 ± 1	50 ± 2	15.3 ± 0.9	222 ± 9	6.0 ± 0.2	340 ± 10
14 Jun	1.51 ± 0.05	1.9 ± 0.2	33.8 ± 0.9	15.3 ± 0.2	4.2 ± 0.4	1.47 ± 0.04	42 ± 1	0.59 ± 0.02	152 ± 1	23.24 ± 0.05	19.6 ± 0.2	17.7 ± 0.5	8.7 ± 0.3	98.1 ± 0.9	< 22	< 2.9	68 ± 2	0.78 ± 0.02	240 ± 10
18 Jun	3.2 ± 0.2	2.1 ± 0.2	47 ± 2	9.13 ± 0.04	< SB	1.5 ± 0.1	107.8 ± 0.1	2.4 ± 0.2	1100 ± 200	< SB	42.27 ± 0.05	53 ± 3	52 ± 2	50.7 ± 0.7	31.4 ± 0.3	61 ± 2	103 ± 4	6.6 ± 0.3	220 ± 20
22 Jun	3.1 ± 0.1	15 ± 1	43 ± 1	16.7 ± 0.1	< 0.51	2.1 ± 0.1	32 ± 1	0.37 ± 0.01	< 140	< SB	143.0 ± 0.1	34.4 ± 0.8	31 ± 1	127 ± 2	108 ± 4	< 3.0	143 ± 6	70 ± 4	157 ± 4
26 Jun	5.7 ± 0.1	8.7 ± 0.5	66 ± 2	18.9 ± 0.1	0.63 ± 0.04	2.92 ± 0.08	88 ± 2	3.25 ± 0.05	< 140	0.825 ± 0.007	42.7 ± 0.3	90.9 ± 0.4	11.4 ± 0.7	192 ± 2	32 ± 2	11.8 ± 0.6	460 ± 10	18.9 ± 0.6	144 ± 3
30 Jun	4.36 ± 0.04	13.5 ± 0.1	88 ± 1	8.52 ± 0.08	< SB	4.0 ± 0.2	< 51	6.19 ± 0.07	< 170	< SB	15.1 ± 0.3	99.5 ± 0.7	16.1 ± 0.5	111 ± 2	61 ± 2	380 ± 10	419 ± 7	36.4 ± 0.2	710 ± 30
04 Jul	4.40 ± 0.08	13.9 ± 0.6	112 ± 1	17.7 ± 0.1	0.87 ± 0.05	3.1 ± 0.2	42.6 ± 0.8	6.7 ± 0.2	< 140	4.19 ± 0.04	8.0 ± 0.2	108 ± 1	21.9 ± 0.7	93 ± 3	37 ± 2	412 ± 6	200 ± 3	16.1 ± 0.3	500 ± 40
08 Jul	2.1 ± 0.2	2.2 ± 0.4	< 38	13.9 ± 0.1	< 0.51	2.07 ± 0.04	< 42	3.1 ± 0.7	1100 ± 300	1.44 ± 0.01	18.90 ± 0.02	69 ± 2	15.0 ± 0.7	207 ± 2	42 ± 1	2.75 ± 0.02	160 ± 10	25.3 ± 0.2	< 47
12 Jul	62.2 ± 0.9	14.3 ± 0.9	1020 ± 20	68 ± 1	< SB	15.0 ± 0.3	49 ± 3	56.2 ± 0.8	38 ± 3	23.8 ± 0.1	28.1 ± 0.4	1320 ± 20	69 ± 1	233 ± 2	109 ± 4	338 ± 6	2610 ± 60	57 ± 1	1150 ± 30
16 Jul	36.6 ± 0.1	10.7 ± 0.9	701 ± 9	56 ± 1	2.1 ± 0.1	11.5 ± 0.3	88 ± 7	34.6 ± 0.5	63 ± 2	43.4 ± 0.4	14.5 ± 0.5	870 ± 20	101 ± 2	203 ± 4	312 ± 9	460 ± 20	1330 ± 20	30 ± 1	1000 ± 30
20 Jul	2.16 ± 0.02	4.1 ± 0.6	< 36	3.75 ± 0.02	< 0.49	0.96 ± 0.07	< 41	2.57 ± 0.04	< 140	< SB	15.5 ± 0.1	35.1 ± 0.4	75 ± 2	50.3 ± 0.6	< 22	< 2.9	47 ± 1	1.26 ± 0.03	< 45
24 Jul	6.0 ± 0.3	4.4 ± 0.3	64 ± 1	16.42 ± 0.03	< SB	2.62 ± 0.06	42 ± 1	3.26 ± 0.09	< 140	< SB	27.2 ± 0.1	75.0 ± 0.2	87 ± 2	88.3 ± 0.9	96 ± 4	< 3.0	195 ± 5	45 ± 1	255 ± 7
28 Jul	6.37 ± 0.06	43 ± 4	74 ± 2	15.5 ± 0.1	14.5 ± 0.8	4.3 ± 0.2	131 ± 8	4.7 ± 0.2	1100 ± 20	< SB	48.39 ± 0.04	86 ± 9	28.0 ± 0.7	30.6 ± 0.3	106 ± 4	159 ± 5	2200 ± 200	38 ± 2	520 ± 20
05 Aug	3.99 ± 0.09	4.9 ± 0.3	116 ± 2	25.5 ± 0.3	< 0.55	1.37 ± 0.08	< 45	2.92 ± 0.01	< 150	3.08 ± 0.02	44.29 ± 0.04	55 ± 1	85 ± 2	68.5 ± 0.6	17.7 ± 0.9	< 3.3	147 ± 4	4.07 ± 0.02	270 ± 10
09 Aug	6.22 ± 0.05	0.25 ± 0.01	37 ± 1	29.9 ± 0.4	< 0.53	2.58 ±0.07	< 44	2.6 ± 0.3	1210 ± 50	1.83 ± 0.02	7.79 ± 0.04	47 ± 1	123 ± 6	327 ± 8	90 ± 1	12 ± 1	80 ± 10	2.44 ± 0.03	343 ± 20
13 Aug	18.3 ± 0.8	11.9 ± 0.6	109 ± 2	26.4 ± 0.1	0.8 ± 0.2	4.9 ± 0.1	84 ± 5	9.0 ± 0.4	1200 ± 100	3.71 ± 0.06	13.2 ± 0.5	210 ± 20	32 ± 2	225 ± 2	< 22	62.7 ± 0.8	720 ± 70	25.9 ± 0.2	194 ± 6
17 Aug	3.03 ± 0.07	40 ± 1	77 ± 1	16.6 ± 0.1	1.22 ± 0.09	3.06 ± 0.06	88 ± 6	2.69 ± 0.02	30.8 ± 0.5	< SB	5.6 ± 0.2	53.8 ± 0.5	5.3 ± 0.4	78 ± 2	41 ± 2	124 ± 2	130 ± 3	11.3 ± 0.2	232 ± 8
21 Aug	0.812 ± 0.007	3.5 ± 0.1	< 35	5.73 ± 0.07	< 0.46	0.55 ± 0.04	< 38	0.683 ± 0.008	< 130	< SB	12.1 ± 0.1	15.6 ± 0.2	4.4 ± 0.2	84 ± 2	< 21	< 2.8	27.9 ± 0.7	0.84 ± 0.05	< 43
25 Aug	0.298 ± 0.008	< 0.31	< 35	7.4 ± 0.1	6.3 ± 0.3	2.4 ± 0.4	42 ± 2	0.57 ± 0.06	190 ± 10	0.907 ± 0.007	41.60 ± 0.03	< 16	5.2 ± 0.4	25.1 ± 0.4	< 21	< 2.8	< 30	< 0.32	< 44
29 Aug	0.527 ± 0.006	5.9 ± 0.6	< 39	10.1 ± 0.2	< 0.53	0.60 ± 0.06	< 44	2.09 ± 0.03	< 150	< SB	35.5 ± 0.1	19.2 ± 0.1	4.8 ± 0.2	88 ± 2	57 ± 5	< 3.1	43.1 ± 0.9	0.78 ± 0.01	< 49
02 Sep	4.9 ± 0.1	5.9 ± 0.3	86 ± 3	21.2 ± 0.1	< SB	3.80 ± 0.04	44 ± 4	6.7 ± 0.3	0.11 ± 0.01	2.36 ± 0.03	12.6 ± 0.3	125 ± 2	5.4 ± 0.3	183 ± 1	39 ± 3	380 ± 20	640 ± 30	17.0 ± 0.6	98 ± 4
06 Sep	26.7 ± 0.9	3.8 ± 0.2	177 ± 5	68.0 ± 0.4	< SB	14.1 ± 0.6	110 ± 10	17.9 ± 0.6	1100 ± 100	26.6 ± 0.2	12 ± 2	460 ± 10	8.6 ± 0.3	930 ± 10	159 ± 7	22.1 ± 0.2	1700 ± 100	64 ± 1	380 ± 10
10 Sep	0.315 ± 0.005	< 0.41	< 46	10.76 ± 0.05	< 0.62	4.8 ± 0.4	41 ± 2	0.55 ± 0.09	< 170	0.489 ± 0.005	4.73 ± 0.07	< 21	3.8 ± 0.2	29.0 ± 0.1	< 28	29.6 ± 0.7	< 39	< 0.41	440 ± 30

SB = Sample Blank. Values below the LOD were obtained by using the real solution volume and air volume of each sample.

Supplementary Table 2. Lanthanide concentrations determined in PM_{10} samples collected in a) 2011; b) 2012; c) 2013.

a) **2011 CAMPAIGN**

Start date	La (fg/m^3)	Ce (fg/m^3)	Pr (fg/m^3)	Nd (fg/m^3)	Sm (fg/m^3)	Eu (fg/m^3)	Gd (fg/m^3)	Tb (fg/m^3)	Dy (fg/m^3)	Ho (fg/m^3)	Er (fg/m^3)	Yb (fg/m^3)
29 Mar	930 ± 70	1180 ± 40	189 ± 5	760 ± 20	157 ± 6	37.8 ± 0.9	200 ± 20	15 ± 1	110 ± 6	3.3 ± 0.1	47 ± 4	38 ± 3
03 Apr	1640 ± 30	4100 ± 200	360 ± 10	1370 ± 20	270 ± 10	62 ± 4	336 ± 6	37 ± 1	220 ± 10	24.8 ± 0.3	104 ± 5	79 ± 2
07 Apr	1740 ± 60	2850 ± 70	383 ± 4	1440 ± 30	300 ± 10	58 ± 2	290 ± 10	33 ± 3	195 ± 8	21.2 ± 0.8	77 ± 6	54 ± 2
11 Apr	< 10	247 ± 9	< 3.6	< 15	< 4.1	< 5.7	< 5.9	3.9 ± 0.2	11.8 ± 0.8	14.9 ± 0.9	21 ± 2	23 ± 2
01 May	620 ± 20	313 ± 6	201 ± 5	542 ± 6	163 ± 7	93 ± 5	176 ± 7	83 ± 6	134 ± 4	69 ± 2	92 ± 5	82 ± 3
05 May	2020 ± 40	3090 ± 60	531 ± 8	1660 ± 40	430 ± 20	190 ± 4	410 ± 10	150 ± 3	320 ± 10	131 ± 6	200 ± 10	182 ± 6
09 May	820 ± 30	3100 ± 100	440 ± 20	610 ± 30	380 ± 20	300 ± 10	370 ± 20	270 ± 20	280 ± 20	260 ± 20	240 ± 20	240 ± 20
13 May	1520 ± 60	11400 ± 400	353 ± 9	1350 ± 20	280 ± 30	77 ± 1	340 ± 10	39.7 ± 0.6	184 ± 2	21.8 ± 0.7	82 ± 2	66 ± 4
17 May	1600 ± 60	2400 ± 70	360 ± 10	1300 ± 20	286 ± 5	71 ± 2	280 ± 20	35.0 ± 0.5	170 ± 10	23 ± 2	73 ± 5	59 ± 4
21 May	250 ± 9	350 ± 10	60 ± 3	230 ± 10	47 ± 3	< 14	48 ± 3	14.7 ± 0.9	30 ± 2	27 ± 2	21 ± 2	8.9 ± 0.7
25 May	430 ± 20	330 ± 10	93 ± 3	400 ± 10	69 ± 5	13 ± 1	43 ± 4	< 2.0	52.8 ± 0.9	< 1.4	13 ± 1	8.0 ± 0.6
29 May	208 ± 3	< 130	61 ± 2	200 ± 10	48 ± 1	39 ± 2	37 ± 4	18.7 ± 0.2	40 ± 3	18 ± 1	27 ± 2	27 ± 3
05 Jun	393 ± 8	3200 ± 100	111 ± 3	370 ± 10	98 ± 5	51 ± 2	105 ± 8	22 ± 1	60 ± 4	19.6 ± 0.6	39 ± 6	33 ± 1
09 Jun	760 ± 20	900 ± 10	175 ± 7	650 ± 50	130 ± 10	73 ± 2	150 ± 10	20 ± 1	86 ± 9	18 ± 2	39 ± 4	37 ± 9
13 Jun	2530 ± 90	4200 ± 200	620 ± 30	2400 ± 100	570 ± 30	186 ± 8	610 ± 40	136 ± 8	390 ± 20	103 ± 6	200 ± 20	150 ± 10
17 Jun	1149 ± 9	4100 ± 100	249 ± 8	920 ± 30	195 ± 9	67 ± 4	220 ± 10	35 ± 3	130 ± 10	24 ± 2	71 ± 6	54 ± 7
21 Jun	161 ± 5	< 140	30 ± 3	88 ± 6	19 ± 2	34.5 ± 0.7	35 ± 4	7.9 ± 0.2	18 ± 2	5.7 ± 0.7	22 ± 1	9.3 ± 0.9
25 Jun	197 ± 6	260 ± 20	72 ± 2	220 ± 10	60 ± 4	45 ± 2	88 ± 8	15 ± 0.7	46 ± 2	16 ± 0.6	30 ± 4	30 ± 2
29 Jun	220 ± 20	298 ± 8	67 ± 4	230 ± 10	45 ± 3	27 ± 2	59 ± 3	8.7 ± 0.6	35 ± 4	15 ± 3	28 ± 2	18 ± 1
03 Jul	350 ± 10	400 ± 10	80 ± 2	240 ± 10	55 ± 5	40 ± 1	67 ± 7	10.9 ± 0.6	35 ± 3	10.8 ± 0.9	24 ± 1	21 ± 1
07 Jul	330 ± 10	450 ± 30	121 ± 7	340 ± 30	94 ± 2	72 ± 6	129 ± 7	53 ± 3	80 ± 7	50 ± 5	67 ± 6	54 ± 3
15 Jul	38 ± 1	1380 ± 80	17 ± 1	49 ± 3	< 12	18.2 ± 0.6	19.9 ± 0.5	3.5 ± 0.3	8 ± 1	1.60 ± 0.01	6.4 ± 0.3	14 ± 1
19 Jul	127 ± 6	170 ± 20	55 ± 7	120 ± 10	38 ± 3	45 ± 2	45.4 ± 0.8	26 ± 1	30 ± 1	26 ± 1	29 ± 3	26 ± 3
23 Jul	440 ± 20	620 ± 20	100 ± 10	380 ± 30	70 ± 4	45 ± 3	92 ± 3	17 ± 3	51 ± 2	9.9 ± 0.2	32 ± 3	19 ± 2

Values below the LOD were obtained by using the real solution volume and air volume of each sample.

b) **2012 CAMPAIGN**

Start date	La (fg/m^3)	Ce (fg/m^3)	Pr (fg/m^3)	Nd (fg/m^3)	Sm (fg/m^3)	Eu (fg/m^3)	Gd (fg/m^3)	Tb (fg/m^3)	Dy (fg/m^3)	Ho (fg/m^3)	Er (fg/m^3)	Yb (fg/m^3)
17 Apr	1680 ± 70	3500 ± 200	360 ± 20	1440 ± 90	271 ± 7	94 ± 7	260 ± 30	42 ± 1	196 ± 9	33 ± 2	101 ± 7	84 ± 6
21 Apr	1150 ± 50	2600 ± 100	270 ± 20	1110 ± 60	219 ± 8	70 ± 3	230 ± 10	34.7 ± 0.9	156 ± 8	27.1 ± 0.4	78 ± 5	61 ± 5
25 Apr	1170 ± 30	8700 ± 100	261 ± 8	1010 ± 50	200 ± 20	93 ± 6	230 ± 7	33 ± 2	144 ± 6	26 ± 1	77 ± 3	67 ± 5
29 Apr	1340 ± 30	3100 ± 100	323 ± 9	1220 ± 30	240 ± 20	79 ± 6	250 ± 10	42 ± 2	183 ± 9	34 ± 3	89 ± 6	76 ± 7
03 May	1040 ± 90	2160 ± 70	230 ± 7	910 ± 40	350 ± 30	58 ± 5	190 ± 10	24 ± 2	130 ± 10	18.9 ± 0.5	66 ± 5	56 ± 5
07 May	1830 ± 70	12200 ± 500	435 ± 3	1640 ± 60	330 ± 10	85 ± 3	390 ± 20	54 ± 2	230 ± 7	37 ± 2	119 ± 3	96 ± 4
11 May	1700 ± 100	3500 ± 100	388 ± 7	1490 ± 50	294 ± 9	81 ± 4	290 ± 10	48 ± 1	189 ± 6	32 ± 1	92 ± 4	87 ± 4
15 May	3400 ± 100	9300 ± 500	806 ± 2	2790 ± 80	570 ± 30	144 ± 7	610 ± 20	94.3 ± 0.8	410 ± 10	66.9 ± 0.4	194 ± 7	160 ± 10
19 May	2160 ± 50	5000 ± 200	550 ± 20	2030 ± 60	430 ± 20	114 ± 5	430 ± 10	69 ± 4	310 ± 20	48.5 ± 0.1	158 ± 4	130 ± 10
23 May	1640 ± 30	3500 ± 100	380 ± 8	1380 ± 20	270 ± 20	76 ± 3	280 ± 20	39 ± 1	216 ± 9	36 ± 2	100 ± 30	100 ± 10
27 May	1040 ± 40	1900 ± 40	190 ± 10	850 ± 30	160 ± 20	48 ± 3	162 ± 5	25 ± 2	110 ± 10	15.8 ± 0.4	52 ± 5	45 ± 3
31 May	700 ± 50	8400 ± 100	162 ± 4	700 ± 100	140 ± 20	51 ± 8	150 ± 20	26 ± 6	97 ± 6	18 ± 4	47 ± 3	51 ± 6
04 Jun	880 ± 90	1980 ± 50	207 ± 7	770 ± 30	170 ± 10	49 ± 3	134 ± 3	21.9 ± 0.2	111 ± 8	16 ± 1	55 ± 5	51 ± 4
08 Jun	730 ± 60	1290 ± 30	131 ± 6	471 ± 9	107 ± 7	40 ± 2	100 ± 20	14.5 ± 0.4	77 ± 4	10 ± 1	33 ± 3	29 ± 2
12 Jun	1800 ± 100	7700 ± 300	373 ± 3	1490 ± 50	310 ± 20	79 ± 3	310 ± 20	47 ± 2	210 ± 7	33 ± 2	102 ± 3	110 ± 30
16 Jun	510 ± 20	1200 ± 100	120.2 ± 0.7	420 ± 20	86 ± 6	34 ± 3	84 ± 5	12.23 ± 0.07	62 ± 3	10 ± 1	32 ± 3	28 ± 2
20 Jun	620 ± 30	1330 ± 50	124 ± 7	490 ± 10	90 ± 10	32 ± 2	107 ± 8	14.3 ± 0.7	65 ± 5	8.3 ± 0.2	37 ± 4	29 ± 2
24 Jun	90 ± 20	350 ± 30	25 ± 3	80 ± 4	13 ± 2	19 ± 1	< 14	< 1.6	< 6.8	< 1.2	5.3 ± 0.4	13 ± 2
28 Jun	277 ± 5	750 ± 30	66 ± 4	227 ± 9	40 ± 10	30 ± 10	43 ± 4	8 ± 3	30 ± 5	4 ± 2	16 ± 3	26 ± 3
02 Jul	840 ± 50	1890 ± 80	200 ± 10	750 ± 20	132 ± 6	44 ± 3	120 ± 10	21 ± 1	104 ± 9	14 ± 1	45 ± 5	40 ± 2
06 Jul	1600 ± 100	3300 ± 100	374 ± 9	1470 ± 50	280 ± 10	66 ± 4	303 ± 5	41 ± 1	187 ± 7	30 ± 2	89 ± 3	74 ± 7
10 Jul	2330 ± 80	5100 ± 100	606 ± 9	2240 ± 70	490 ± 30	108 ± 5	460 ± 40	80 ± 30	340 ± 20	56 ± 6	153 ± 9	120 ± 10
14 Jul	850 ± 40	11200 ± 100	207 ± 8	730 ± 20	140 ± 10	45 ± 2	159 ± 8	20.2 ± 0.8	90 ± 6	12.6 ± 0.8	43 ± 3	50 ± 2
18 Jul	1410 ± 40	2830 ± 90	316 ± 9	1140 ± 40	230 ± 10	60 ± 3	200 ± 20	32 ± 2	150 ± 10	24.7 ± 0.6	79 ± 3	80 ± 7
22 Jul	2300 ± 200	9000 ± 1000	300 ± 20	1240 ± 50	301 ± 6	74 ± 7	270 ± 20	30 ± 10	180 ± 20	25 ± 4	76 ± 7	63 ± 5
26 Jul	2100 ± 100	4870 ± 70	520 ± 20	2020 ± 40	380 ± 10	114 ± 8	400 ± 20	61 ± 8	249 ± 6	40 ± 2	112 ± 5	90 ± 10
30 Jul	500 ± 20	9400 ± 200	121 ± 5	460 ± 20	81 ± 2	27 ± 1	102 ± 7	15 ± 2	68 ± 3	12 ± 2	31 ± 1	37 ± 4
03 Aug	170 ± 20	460 ± 30	36 ± 3	147 ± 7	26 ± 4	22 ± 2	28 ± 2	4.9 ± 0.2	22 ± 6	1.6 ± 0.2	10 ± 1	25 ± 3
07 Aug	480 ± 30	1230 ± 40	110 ± 10	410 ± 20	80 ± 8	37 ± 2	93 ± 7	13.0 ± 0.5	63 ± 6	10.5 ± 0.9	35 ± 3	36 ± 2
11 Aug	170 ± 20	16300 ± 400	43 ± 1	143 ± 9	28 ± 5	19 ± 1	58 ± 3	5.7 ± 0.8	19 ± 2	2.8 ± 0.5	9.9 ± 0.9	9.4 ± 0.9
15 Aug	390 ± 20	930 ± 40	86 ± 4	540 ± 20	77 ± 5	29 ± 2	79 ± 8	10.2 ± 0.6	64 7	8.01 ± 0.05	31 ± 2	25 ± 3
19 Aug	1030 ± 70	2300 ± 100	248 ± 6	920 ± 30	170 ± 10	48 ± 2	170 ± 20	25 ± 1	121 ± 8	16.5 ± 0.9	53 ± 7	51 ± 3
23 Aug	690 ± 30	1700 ± 60	169 ± 2	650 ± 20	130 ± 10	41 ± 2	117 ± 6	22 ± 1	117 ± 8	19 ± 2	56 ± 5	51 ± 4
27 Aug	390 ± 20	9700 ± 400	85 ± 1	370 ± 10	76 ± 4	26 ± 2	112 ± 5	10.7 ± 0.4	59 ± 5	7.4 ± 0.8	27 ± 3	25 ± 2
31 Aug	450 ± 30	1030 ± 30	109 ± 2	385 ± 9	70 ± 3	27 ± 1	62 ± 2	8.7 ± 0.6	51 ± 4	8 ± 1	24.5 ± 0.6	29 ± 2
04 Sep	240 ± 10	12700 ± 300	63 ± 4	206 ± 7	34 ± 2	24 ± 1	92 ± 7	8.7 ± 0.5	27 ± 3	3.9 ± 0.6	17 ± 2	31 ± 3

c) **2013 CAMPAIGN**

Start date	La (fg/m^3)	Ce (fg/m^3)	Pr (fg/m^3)	Nd (fg/m^3)	Sm (fg/m^3)	Eu (fg/m^3)	Gd (fg/m^3)	Tb (fg/m^3)	Dy (fg/m^3)	Ho (fg/m^3)	Er (fg/m^3)	Yb (fg/m^3)
01 May	1600 ± 100	1220 ± 30	450 ± 10	910 ± 30	311 ± 10	77 ± 3	310 ± 20	49 ± 3	250 ± 20	38.7 ± 0.7	110 ± 6	91 ± 6
05 May	2260 ± 30	2000 ± 100	640 ± 10	1320 ± 40	423 ± 30	115 ± 5	410 ± 20	74 ± 1	310 ± 10	61.4 ± 0.8	150 ± 10	118 ± 6
09 May	9100 ± 300	< 100	61 ± 2	< 32	54 ± 7	36 ± 3	67 ± 3	20 ± 2	41 ± 1	21.1 ± 0.9	25.1 ± 0.3	19 ± 3
13 May	1360 ± 20	1090 ± 60	410 ± 10	750 ± 10	256 ± 20	67 ± 5	257 ± 8	39 ± 1	180 ± 10	36 ± 1	85 ± 2	69.0 ± 0.5
17 May	1020 ± 40	2180 ± 70	270 ± 30	1100 ± 20	214 ± 10	49 ± 3	173 ± 6	30 ± 1	160 ± 10	29 ± 2	80 ± 5	65 ± 4
21 May	760 ± 10	500 ± 10	223 ± 7	340 ± 20	157 ± 3	49 ± 2	169 ± 7	24 ± 2	124 ± 7	24 ± 1	67 ± 3	44 ± 2
25 May	280 ± 10	500 ± 20	67 ± 2	290 ± 20	982 ± 40	20 ± 1	< 15	18 ± 2	36 ± 4	8.1 ± 0.7	17 ± 1	31 ± 6
29 May	490 ± 20	195 ± 4	143 ± 8	53 ± 2	89 ± 3	35 ± 1	102 ± 8	11.7 ± 0.8	68 ± 2	14.4 ± 0.6	36 ± 3	27.1 ± 0.6
02 Jun	740 ± 30	510 ± 10	194 ± 8	190 ± 8	138 ± 2	44 ± 2	141 ± 5	22 ± 2	125 ± 3	17 ± 1	54 ± 4	46 ± 2
06 Jun	3010 ± 70	6000 ± 300	730 ± 20	2590 ± 50	508 ± 10	113 ± 3	440 ± 10	76 ± 8	371 ± 8	72 ± 3	176 ± 9	170 ± 10
10 Jun	880 ± 40	730 ± 20	282 ± 5	460 ± 10	188 ± 3	45 ± 2	200 ± 10	26 ± 1	134.9 ± 0.6	21.6 ± 0.4	71 ± 8	54 ± 2
14 Jun	< 22	< 103	17.2 ± 0.7	< 33	14 ± 1	< 10	14 ± 2	< 1.5	20 ± 2	3.4 ± 0.2	16.1 ± 0.4	12 ± 2
18 Jun	< 21	< 99	< 7.6	< 32	< 8.6	< 10	< 12	< 1.4	< 5.9	< 1.0	< 3.0	< 3.5
22 Jun	300 ± 20	< 110	90 ± 2	< 35	57 ± 3	20.1 ± 0.7	64 ± 3	7.9 ± 0.3	49 ± 3	6.8 ± 0.6	27.0 ± 0.8	13.5 ± 0.6
26 Jun	820 ± 70	620 ± 20	266 ± 5	430 ± 20	166 ± 9	57 ± 5	187 ± 5	29 ± 3	145 ± 4	26.5 ± 0.1	72 ± 3	54.7 ± 0.9
30 Jun	1700 ± 200	889 ± 2	350 ± 10	470 ± 20	257 ± 20	153 ± 7	246 ± 9	120 ± 4	217 ± 8	117 ± 5	143 ± 5	150 ± 5
04 Jul	2100 ± 100	1390 ± 20	900 ± 30	1040 ± 20	695 ± 20	630 ± 40	632 ± 9	510 ± 10	620 ± 30	457 ± 8	520 ± 40	460 ± 10
08 Jul	300 ± 30	549 ± 6	70 ± 4	330 ± 20	52 ± 3	18 ± 1	< 13	4.0 ± 0.2	39 ± 1	5.8 ± 0.3	18.8 ± 0.7	9.4 ± 0.4
12 Jul	17300 ± 400	19700 ± 500	3900 ± 100	14600 ± 400	2651 ± 40	960 ± 40	2690 ± 50	595 ± 4	1790 ± 20	480 ± 30	975 ± 4	810 ± 30
16 Jul	9400 ± 500	12100 ± 700	2600 ± 100	9210 400	1734 ± 20	780 ± 20	1820 ± 40	306 ± 3	1190 ± 30	244 ± 8	690 ± 30	580 ± 9
20 Jul	76.8 ± 0.5	< 100	49.5 ± 0.4	< 33	29.2 ± 0.4	< 10	52 ± 3	< 1.5	15.2 ± 0.9	2.5 ± 0.2	10.7 ± 0.8	12.6 ± 0.7
24 Jul	490 ± 20	110 ± 8	121 ± 6	< 34	84 ± 2	25 ± 2	98 ± 3	10.7 ± 0.8	57 ± 5	11.8 ± 0.9	29.8 ± 0.3	15.1 ± 0.8
28 Jul	3300 ± 100	3100 ± 100	360 ± 20	1150 ± 60	241 ± 8	82 ± 6	178 ± 9	61 ± 3	167 ± 9	65 ± 3	110 ± 10	79 ± 4
05 Aug	176 ± 7	< 110	90 ± 8	< 37	64 ± 4	33 ± 1	70 ± 4	9.2 ± 0.8	68 ± 3	14 ± 1	41 ± 1	28.2 ± 0.8
09 Aug	28500 ± 400	53000 ± 2000	118 ± 8	282 ± 7	56 ± 8	43 ± 3	250 ± 30	18.2 ± 0.3	29.0 ± 0.8	14 ± 5	12 ± 1	9 ± 2
13 Aug	1690 ± 60	3480 ± 70	409 ± 8	1530 ± 60	287 ± 10	55 ± 1	200 ± 10	33 ± 2	180 ± 10	29 ± 2	90 ± 6	68 ± 4
17 Aug	300 ± 20	< 100	82 ± 3	< 33	68 ± 3	14.7 ± 0.2	86 ± 9	13.18 ± 0.07	56 ± 8	10.3 ± 0.3	26 ± 2	10.1 ± 0.7
21 Aug	< 20	< 97	< 7.5	< 31	9.4 ± 0.3	< 10	< 12	< 1.4	9.8 ± 0.6	< 1.0	< 3.0	< 3.4
25 Aug	25 ± 1	< 100	28 ± 2	< 32	15 ± 1	< 10	22 ± 1	< 1.4	11.1 ± 0.1	3.1 ± 0.2	7.5 ± 0.8	15 ± 2
29 Aug	< 23	< 110	< 9	< 36	< 10	< 11	< 14	< 1.6	6.1 ± 0.3	< 1.1	< 3.4	< 3.9
02 Sep	400 ± 20	350 ± 10	163 ± 6	166 ± 8	165 ± 2	57.6 ± 0.9	145 ± 6	30 ± 2	160 ± 20	30 ± 2	86 ± 4	73 ± 7
06 Sep	3150 ± 20	6670 ± 80	760 ± 30	2870 ± 60	556 ± 30	125 ± 4	490 ± 20	82.8 ± 0.6	450 ± 20	80 ± 2	250 ± 4	203 ± 8
10 Sep	118 ± 4	< 130	112 ± 2	< 42	72 ± 5	19 ± 1	79 ± 5	6.8 ± 0.2	51 ± 3	12.0 ± 0.8	26 ± 3	22 ± 2

Values below the LOD were obtained by using the real solution volume and air volume of each sample.

Supplementary Table 3. Summary of multiple pairwise comparisons obtained with Kruskal-Wallis and Conover-Iman tests: a) comparison of sampling campaigns; b) comparison of sampling seasons. Letter B identifies campaigns (or seasons) presenting mean of ranks significantly higher than the ones obtained for campaigns (or seasons) identified by letter A; the same concept applies to letter C with respect to letter B.

a) Campaign	Group	Elements
2010, 2011, 2012, 2013	A	Al, Ba, Ca, Co, Ho*, K, Mg*, Mn, Na, Nd, Ni, Pb, V, Zn
2010	A	Cu
2011, 2012, 2013	B	
2011	A	Ti
2010, 2012, 2013	B	
2011	A	La
2013	AB	
2012	B	
2010	C	
2013	A	Fe
2011, 2012	AB	
2010	B	
2011, 2012	A	Mo
2010, 2013	B	
2011, 2013	A	Ce
2010, 2012	B	
2012, 2013	A	Cd
2011	AB	
2010	B	
2012, 2013	A	As
2010	AB	
2011	B	
2011, 2012, 2013	A	Dy, Er, Eu, Gd, Pr, Sm, Tb, Yb
2010	B	

** Mg and Ho were not analysed in samples collected during 2010 campaign.*

b) Season	Group	Elements
Summer, spring	A	As, Ba, Ce, Co, Dy, Er, Eu, Fe, Gd, Ho, K, La, Mg, Mo, Na, Nd, Ni, Pr, Sm, Tb, Ti, Yb, Zn
Summer	A	Al, Ca, Cd, Cu, Mn, Pb
Spring	B	
Spring	A	V
Summer	B	

Supplementary Figure 1. Principal Component Analysis (PC3 vs. PC4) for 2012 samples: a) score plot; b) loading plot.